Myopic Optic Neuropathy

25

Richard F. Spaide and Kyoko Ohno-Matsui

Nearly every feature of the eye is influenced by the development of high myopia. For some structures, such as the sclera, there are well-established abnormalities that have been evaluated in humans, and our knowledge has been amplified by experiments using multiple animal models. For others, the changes associated with high myopia are less clear. The anatomic changes in the optic nerve head and surrounding structures are readily evident by imaging, but the functional changes induced, and the possible pathophysiologic mechanisms are not clearly understood or defined. Ocular imaging is improving rapidly and has provided clues suggesting there may be classes of abnormalities in optic nerve structure and function in high myopia. This chapter explores possible abnormalities of the optic nerve associated with high myopia. Considerations about the possible pathophysiology involved hinges on detailed knowledge of the anatomic and physiology of the optic nerve and associated structures and incorporates analysis of changes induced by high myopia.

25.1 Embryology of the Optic Nerve

The optic vesicle evaginates from the prosencephalon but remains connected by a short optic stalk. Invagination of the optic vesicle forms the optic cup, and the fetal fissure closes not only the optic cup but also the optic stalk. The hyaloid artery and vein enters the stalk medially and continues into the eye to come into contact with the primary vitreous. The hyaloid artery exits the hyaloid canal on the inner aspect of the disc. Between the sixth and seventh weeks, the fissure in the optic stalk, called the choroidal fissure, begins to close to form a tube. Failure of closure would lead to an optic nerve coloboma. The retinal nerve fibers converge on the optic disc through a complicated interaction between attractive and repulsive forces acting on their growth [1]. By the seventh week, axons line the inner wall of the lumen of the optic stalk, and by the eighth week, the stalk is filled with axons that extend back to a primitive chiasm. The cells on the inner side of the stalk are destined to form glial cells between the nerve fibers while the external cells form the glial mantle around the nerve. The scleral development is covered in more detail in Chaps. 5 and 8, but the collagen fibers in the sclera develop in a sequence from the front of the eye to back to eventually reach the already formed nerve. There is penetration of the nerve by collagen fibers starting in the fourth month. The lamina cribrosa then develops and is not fully formed until after birth [2]. The meningeal coverings of the optic nerve start to become evident as layers in the 12th week. Myelination of the nerve begins somewhat before the sixth month of gestation.

25.2 Anatomy of the Optic Nerve

In normal eyes, there are approximately 1.2 million non-myelinated nerve fibers converging on the optic canal to leave the eye through the lamina cribrosa. The aggregate of these nerve fibers and the associated glial cells make up the bulk of the optic nerve. These fibers make a nearly 90 degree turn to enter the optic nerve in emmetropes. The internal opening of the optic nerve is defined by the opening in Bruch's membrane and more posteriorly by the opening in the sclera called the optic canal. The portion of the optic nerve internal to the lamina cribrosa is the prelaminar portion of the nerve. Its internal surface is bounded by a layer of collagen and astrocytes called the inner limiting membrane of Elschnig, which is a distinct entity from the internal limiting membrane of the retina. The prelaminar portion of the nerve is composed of nerve fiber bundles separated by an

R. F. Spaide (✉)
Vitreous, Retina, Macula Consultants of New York, New York, NY, USA

K. Ohno-Matsui
Department of Ophthalmology and Visual Science, Tokyo Medical and Dental University, Bunkyo-Ku, Tokyo, Japan
e-mail: k.ohno.oph@tmd.ac.jp

R. F. Spaide et al. (eds.), *Pathologic Myopia*, https://doi.org/10.1007/978-3-030-74334-5_25

almost equal volume of glial cells. At the outer border of the nerve, separating it from the surrounding retina is the intermediary tissue of Kuhnt, and separating it from the choroid is the border tissue of Jacoby. The laminar portion of the nerve is that section passing through the lamina cribrosa. The connective tissue and glial elements of the lamina cribrosa are more prominent in the nasal and temporal quadrants as compared with the inferior and superior ones [3]. The pores within the lamina cribrosa are larger in the inferior and superior quadrants [4]. There is a bow tie-shaped ridge in the lamina cribrosa that extends from the nasal to the temporal side of the optic canal near the horizontal meridian [5]. There appears to be more robust connective tissue support in the lamina in the horizontal meridians than along the inferosuperior axis. This raises interesting questions, since a greater expanse of the globe is exposed to trauma in the horizontal meridians than in the vertical ones. Posterior to the lamina, the optic nerve expands in diameter and becomes myelinated. Within the intraorbital optic nerve, there are also glial cells and blood vessels and connective tissue septae. The optic nerve is covered by pia mater. The subarachnoid space ends in a blind pouch at the scleral border of the eye. The dura mater is continuous with the outer 1/3 of the sclera.

The blood supply of the nerve varies by location and has been the source of disagreement. The nerve fiber layer derives its supply from the central retinal artery. Branches coursing in a centripetal direction may help supply the prelaminar portion of the nerve. The short posterior ciliary vessels supply a perineural arterial ring, often incomplete, called the circle of Zinn-Haller (first described by Zinn [6] in 1755) that is located in the sclera [6–11]. Branches from the circle of Zinn-Haller supply the prelaminar and laminar nerve and anastomose with the adjacent choroidal circulation. Past theories concerning blood flow have proposed direct communication between the choroid and the prelaminar optic nerve [7]. There is controversy about the circle of Zinn-Haller. Blood supply to the nerve (and the posterior choroid) is derived from many short posterior ciliary arteries that converge upon and anastomose around the nerve. This raises the question of whether the so-called circle of Zinn-Haller is a just the manifestation of a group of anastomoses or if it is a separate and distinct structure in its own right [12]. In this chapter the circle of Zinn-Haller will be considered a distinct anatomic structure. The blood drains from the nerve into branches of the central retinal vein.

25.3 Morphometric Characteristics of the Optic Disc in Normal Eyes

Ordinarily the optic nerve is a slightly ovoid structure that had a mean vertical measurement of 1.92 mm by 1.76 mm horizontally in a study of 319 subjects using magnification-corrected morphometry of optic disc photographs [13]. In a study of 60 eye bank eyes, the measurements were 1.88 mm vertically by 1.76 horizontally [14]. These measurements should be viewed as being approximate because the size of the optic disc among studies has shown variation by study, race, and measurement method. The mean disc area in Caucasians ranged from 1.73 mm^2 to 2.63 mm^2, in African Americans 2.46 mm^2 to 2.67 mm^2, and a similarly large range of sizes among various Asian populations (extensively reviewed in reference [15]). Studies seem to indicate African Americans have larger optic disc areas than other races. The cup is a central depression in the optic nerve. A common metric used to gauge the morphology of the optic disc is the cup-to-disc ratio, or cup/disc, the proportion calculated by dividing the diameter of the depression by the diameter of the disc. Although in common usage there are several difficulties with this metric, the diameter of the disc varies by what feature is measured, that is, the color change, elevation change, or the actual canal diameter. The margin of the optic disc as seen by color photography or ophthalmoscopy does not appear to have a consistent anatomic correlate in OCT imaging [15]. The diameter of the depression is a function of what definition is used for "depression" and what the specified height or curve change used is open to contention. The cup/disc varies with age and race. Finally, the cup-to-disc ratio along the vertical axis usually is not the same as the horizontal axis. Using magnification adjusted planimetry, Jonas and coworkers found the mean horizontal cup/disc was 0.39, while the mean vertical ratio was 0.39 [13]. The Rotterdam study of subjects 55 years of age or older using stereoscopic simultaneous optic disc transparencies found a vertical cup/disc of 0.49 and a horizontal cup/disc of 0.40 [16].

Evaluation of the nerve generally starts with appraising the scleral ring to delineate the optic disc size. As they exit the eye, the retinal nerve fibers arch over and create the optic nerve rim. The substance of the prelaminar nerve comprises nerve fibers and glial cells. Although Anderson stated nerve has a large proportion of glial cells [17], the variability of the mix from one person to the next is not known. Monkeys with larger nerve heads were found to have a greater number of retinal nerve fibers [18]. Large optic disc sizes also generally have greater neural rim area, and the number of nerve fibers is increased in larger nerves in humans as well [19]. It is likely that large nerves are not necessarily scaled up versions of smaller ones. Even though the rim area may be larger in bigger optic discs, the cup generally increases in size as well. A normal optic nerve shows varying rim thickness in most eyes known as the ISNT rule in which the order of nerve fiber thickness is from greatest to least inferior, superior, nasal, and temporal. Loss of the rim to include notching is suspicious for associated nerve fiber loss. The optic nerve is a vascular structure and ordinarily has a pinkish-orange color. In a sense, the nerve fibers act like light pipes, and a healthy nerve shows a reflection that has a depth. Loss of

neurons, such as in optic neuropathies, causes the nerve to become pallorous; the reflection is whiter with less depth.

25.4 Optic Nerve Hypoplasia

Optic nerve hypoplasia is the most common congenital abnormality of the optic nerve [20]. The optic nerve appears small, often misshapen, and can be surrounded by a ring of altered pigmentation that is called the double ring sign. The vessels on the nerve often show anomalies as well to include abnormal branching patterns, altered vascular density on the nerve head, and venous dilation. The retinal nerve fiber layer can show a generalized decrease, sector defects, or a combination of the two. Often there are sufficient nerve fibers in the maculopapillary bundle to support nearly normal visual acuity.

25.5 Glaucoma

Glaucoma, the most commonly acquired abnormality of the nerve, shows loss of the retinal nerve fiber layer to a greater extent than age alone would dictate and associated changes in the optic nerve head including changes in the collagen, elastic fibers, and extracellular matrix [21–29]. There is increased cupping of the nerve, tensile expansion, and distortion of load-bearing structures in the eye such as the peripapillary sclera, the scleral canal, and the lamina cribrosa [30–33]. Expansion of the scleral canal, compaction, and posterior displacement of the lamina cribrosa occur in glaucoma. The changes in the lamina cribrosa appear to be the result of more than simple stress-induced strain effects, as biologic remodeling of the lamina occurs [34]. These alterations appear to reverse somewhat following glaucoma surgery [35, 36]. There are lines of evidence that converge on the concept that retinal nerve fiber damage at the level of the lamina cribrosa is an important pathophysiologic mechanism in glaucoma. Since this is the site of biomechanical changes induced by glaucoma, a logical, biologically plausible assumption is that the mechanically induced effects ultimately lead to nerve fiber damage.

25.6 Optic Neuropathies Associated with High Myopia

25.6.1 Overview

The most common ocular finding associated with unilateral high myopia is optic nerve hypoplasia [37]. Conversely high myopia occurs frequently in eyes with optic nerve hypoplasia [38]. This is difficult to explain on the basis of current theories of the development of high myopia, which posits a local effect in the eye as the major cause of myopization. It is possible that yet unnamed syndromes exist to link optic nerve hypoplasia or even smaller-sized optic nerve heads with high myopia, as it does appear to be an association that may be more common than the joint probabilities would indicate [39]. Tilting of the optic nerve is more common in high myopia than among emmetropes [40–43]. Tilting of the nerve is associated with smaller optic discs and also visual field defects [40, 41] (Figs. 25.1 and 25.2). In general though, the size of the optic nerve head increases with the amount of myopic refractive error (after correction for image magnification differences) [16, 44] (Fig. 25.3). Expansion of the scleral canal and the lamina cribrosa occurs with enlargement of the optic nerve head. By Laplace's law, the scleral wall stress would be higher per unit cross-sectional area because of the increased radius of the myopic eye and the thinning of the sclera observed in high myopia. Some myopes develop extremely enlarged optic discs with stretching and flattening of the cup (Figs. 25.4 and 25.5). The course of the optic nerve often is skewed as it courses through the sclera in high myopes. Expansion of the posterior portion of the eye in myopia can be associated with acquired pits of the optic nerve, dehiscences of the lamina cribrosa, expansion of the dural attachment posteriorly with enlargement of the subarachnoid space immediately behind the eye (Figs. 25.6 and 25.7), and expansion of the circle of Zinn-Haller with potential compromise of circulation into the prelaminar portion of the nerve. Potential for both mechanical stressors and circulatory compromise exists in high myopia, and any or all of these factors may influence the health of the nerve. In the remaining portion of this chapter, these potential contributors to optic nerve dysfunction will be discussed.

Glaucoma can represent a particular set of difficulties in high myopia. Because of the induced anatomic changes in high myopia, enlargement of the disc in macrodiscs with flattening of the cup, or distortion of the disc with small cups seen in tilted optic discs being prominent examples, diagnosing glaucoma can be difficult. The problem frequently boils down to deciding if the observed abnormalities are due, at least in part, to glaucoma and then determining if the changes are progressive. If so, the eye is generally treated with modalities to reduce the intraocular pressure. It is possible that myopia may cause progressive abnormalities in the retinal nerve fiber by mechanisms not found in emmetropic eyes. What if these changes are lessened by reducing intraocular pressure? Should these conditions be lumped together with glaucoma? In an analysis of 5277 participants from the National Health and Nutrition Examination Survey data, high myopes were found to have a much higher prevalence of visual field defects than either emmetropes or low myopes even though the self-reported prevalence of glaucoma was the same [45]. Since high myopia is a significant risk factor for the development of glaucoma, Qui and coworkers concluded glaucoma surveillance should be intensified in high

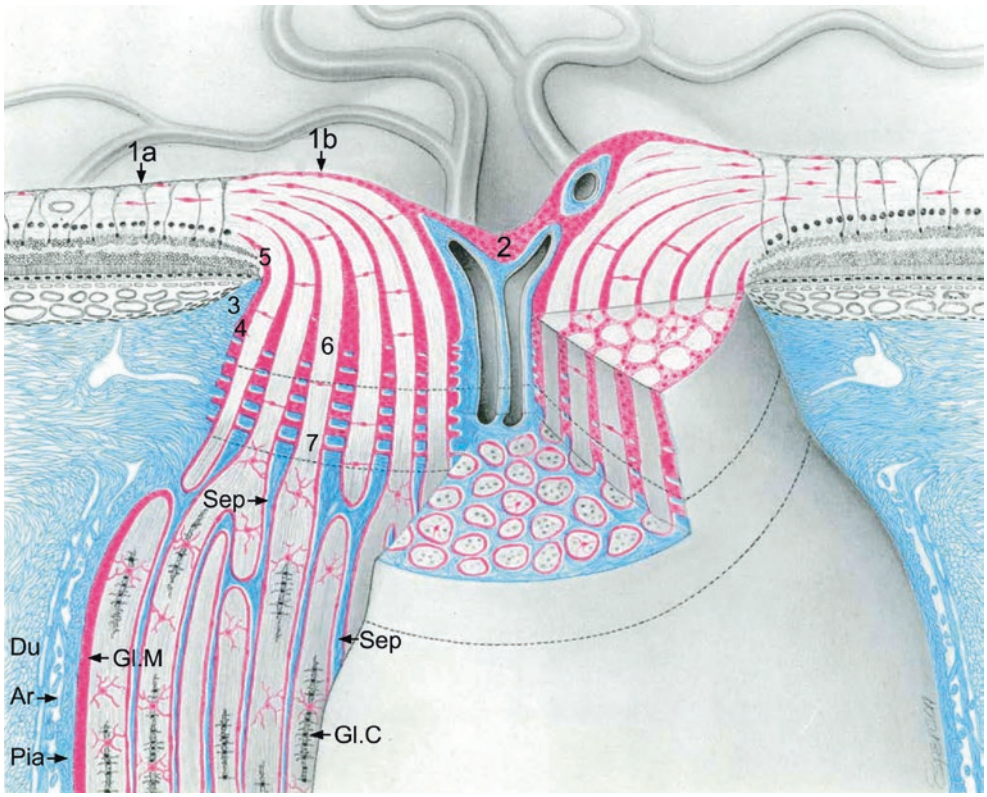

Fig. 25.1 Schematic drawing of the optic nerve in an emmetrope. The numbered regions are as follows: (1a) inner limiting membrane of the retina, (1b) inner limiting membrane of Elschnig, (2) central meniscus of Kuhnt, (3) border tissue of Elschnig, (4) border tissue of Jacoby, (5) intermediary tissue of Kuhnt, (6) anterior portion of lamina cribrosa, and (7) posterior portion of lamina cribrosa. The abbreviations are as follows: Du, dura mater; Ar, arachnoid mater; Pia, pia mater; Gl.M., glial mantle of Fuchs; Gl.C, glial cell; Sep, septae. (From Anderson and Hoyt)

myopes because glaucoma is probably being underdiagnosed in patients with high myopia [45].

Peripapillary atrophy is common in highly myopic eyes. The atrophy is deceptively simple but occurs in zones around the nerve. The outermost region is the alpha zone, which is a region on the outer border of the beta zone and demonstrates irregular pigmentation. The beta zone is a region of loss of the retinal pigment epithelium (RPE). The underlying choroid and sclera are rendered increasingly visible by the absence of the RPE. Further investigation of these eyes with EDI-OCT showed Bruch's membrane stopped short of the optic disc border. The gap between Bruch's membrane and the optic disc border was called the gamma zone [46]. In a histologic evaluation of highly myopic eyes, an area within the gamma zone was identified in which there were no blood vessels >50 μm in diameter. This region was called the delta zone. Alternate terminology has been proposed. The beta zone without Bruch's membrane has been termed βPPA_{-BM}. The beta zone with Bruch's membrane is βPPA_{+BM} [47]. This meanings implied by the expanded nomenclature may be easier to remember.

Rudnicka and Edgar found that increasing size of peripapillary atrophy is associated with decreased global threshold visual field indices [48, 49]. Beta zone peripapillary atrophy, in particular, occurs more commonly in glaucomatous eyes. Glaucomatous visual field progression occurs more rapidly in eyes with a beta zone of peripapillary atrophy [50]. Size of beta zone peripapillary atrophy shows an inverse correlation with neuroretinal rim area and a spatial correlation to visual field loss in glaucoma patients [51].

25.7 Tilted Discs

There are three axes of rotation of an object, and current ophthalmic terminology describing the optic nerve only has terms for two of these. Tilting of the optic nerve refers to one of the horizontal borders of the nerve which are rotated in the transverse plane. Usually the temporal portion of the nerve is posterior to the nasal portion. The optic disc in eyes appears to be smaller than normal; the long axis of the nerve is typically larger, while the horizontal aspect is smaller than a normal disc. This may be related to the underlying structural support of the lamina in which the superior and inferior portions of the lamina appear less robust than the horizontal aspects. The true horizontal width is difficult to measure accurately, however. The visualized width is the true width of the nerve multiplied by the cosine of the angle of posterior rotation. By visual inspection, it is difficult to know what this angle is, but with the advent of optical coherence tomography (OCT), this angle potentially is measurable. However some recent authors estimate the amount of tilt by calculating the ratio between the minimum and maximum diameter of the nerve, a value they termed the index of tilt [52]. This ratio is certainly decreased in tilted optic nerves, but the

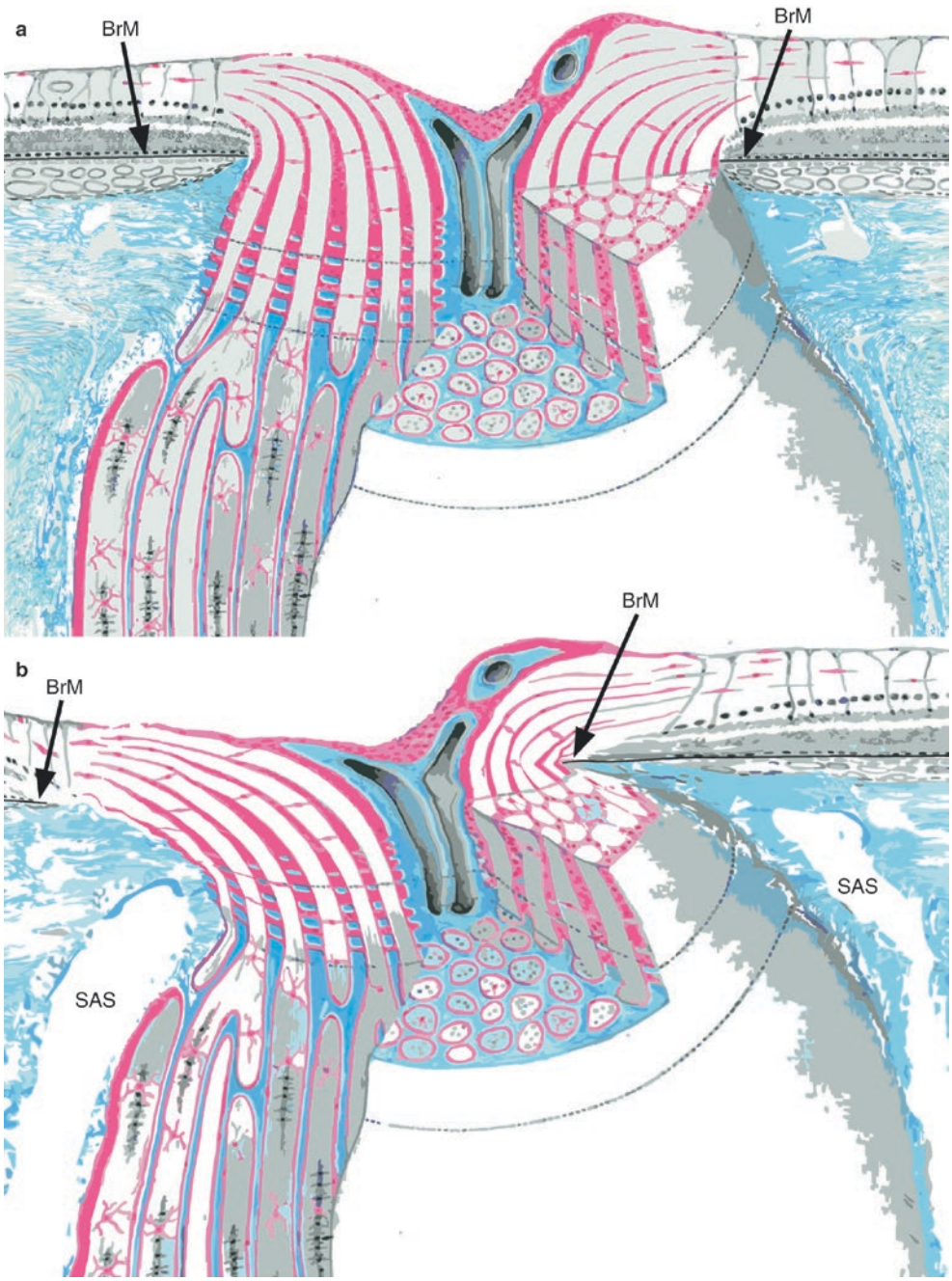

Fig. 25.2 Stylized drawing after Fig. 25.1 showing an emmetropic eye (**a**) and one with a tilted optic disc (**b**). Missing from the drawing in Fig. 25.1 is Bruch's membrane (BrM). The nerve fibers course through the opening in Bruch's membrane, which is centered over the scleral canal. In high myopes with a tilted disc, there is a shifting of the opening in Bruch's membrane temporally. There is a shifting of the inner sclera, which itself is thinned in high myopes. There are thinning of the choroid and absence of the temporal peripapillary choroid. The subarachnoid space (SAS) is expanded

number is not comparable among patients because the minimum width observed in a color photograph is not the true horizontal width. One patient with a very narrow disc with little tilt may have the same index of tilt as another patient with a wider disc but more tilt. In addition, this ratio does not account for vertical elongation of the disc.

Tilted optic discs occur more commonly in myopic eyes but also occur in emmetropic and hyperopic eyes [40–43]. Tilted optic discs also are associated with higher cylindrical errors and longer axial lengths. Intraocular abnormalities associated with tilted optic nerves include smaller optic discs, small optic nerve cups, situs inversus of the retinal vessels, abnormal vascularity on the nerve, and anomalous branching patterns of the retinal vessels in the retina. These associated abnormalities occur in some but not all eyes. Ordinarily a single central retinal artery branches into four arcade vessels, one each supplying the superotemporal, inferotemporal, inferonasal, and superonasal quadrants. In eyes with tilted optic discs, there are often fewer or more vessels branching on the nerve than what is normally seen, and these vessels do not necessarily follow the pattern of the four arcades. On occasions, larger vessels may branch in unusual patterns near the disc in the retina. Some authorities refer to tilted optic discs as congenital tilted optic disc; how-

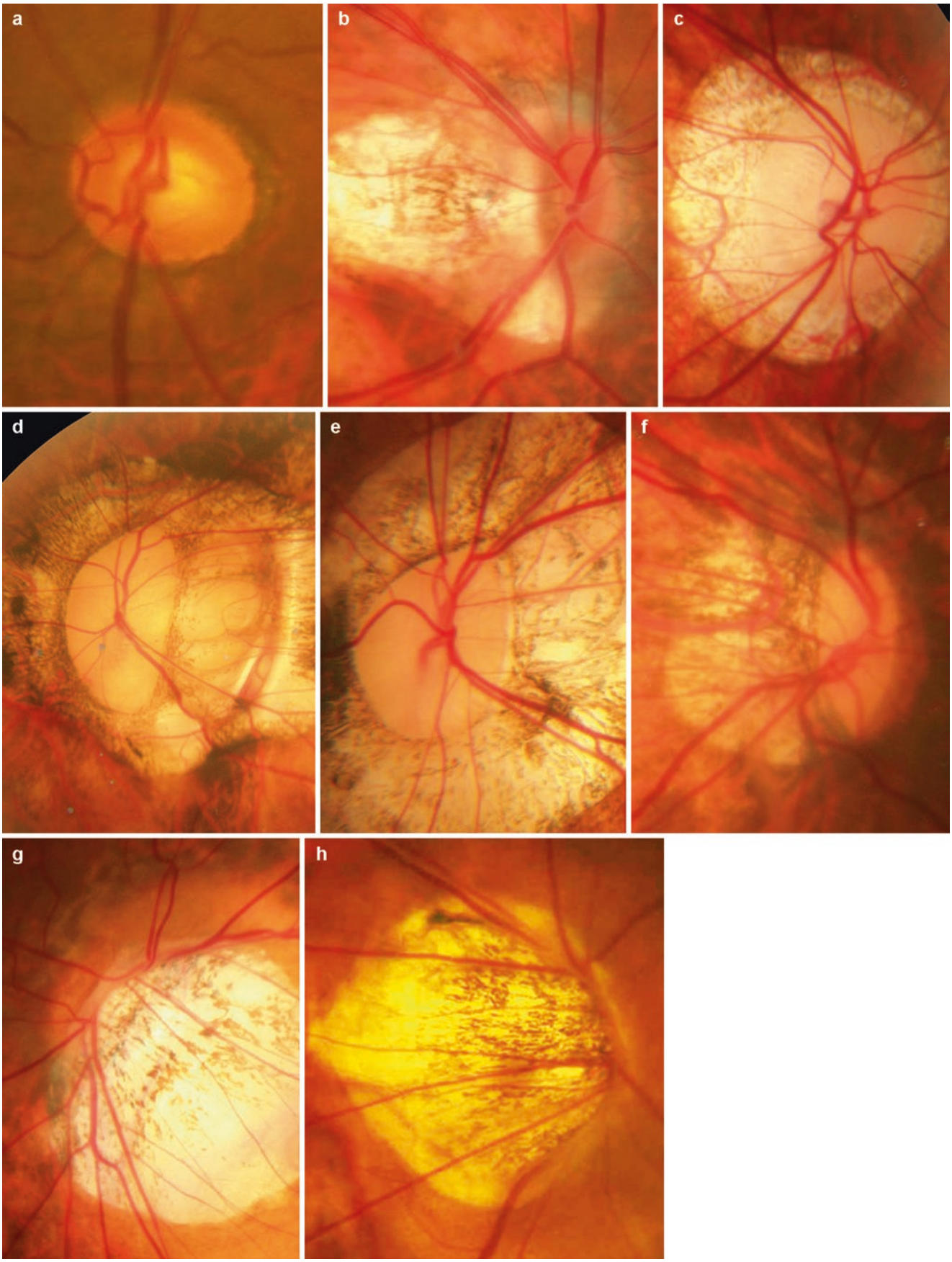
a
b
c
d
e
f
g
h

Fig. 25.3 Optic disc appearance in emmetropic eyes (**a**) and in eyes with pathologic myopia (**b**–**h**). (**a**) A round optic disc in an emmetropic eye (axial length; 23.3 mm) in a 43-year-old woman. The optic disc area is 2.49 mm^2. (**b**) Small optic disc in a highly myopic eye (axial length; 29.0 mm) in a 71-year-old woman. The optic disc area, 0.975 mm^2, was corrected for axial length and corneal curvature, as were all of the other disc areas shown. (**c**–**e**) Various patterns of megalodisc in eyes with pathologic myopia. (**c**) A large and round optic disc with little tilting, torsion, or ovality in the right fundus (axial length; 32.3 mm) of a 29-year-old man. The optic disc area adjusted by an axial length and corneal curvature is 9.57 mm^2. (**d**) A large and oval disc in the left fundus (axial length; 33.0 mm) of a 59-year-old woman. The optic disc area was 5.21 mm^2. (**e**) A large disc in the left fundus (axial length; 35.3 mm) of a 50-year-old woman. The optic disc area corrected for axial length and corneal curvature was 5.09 mm^2. (**f**) A vertically oval disc in the right fundus (axial length; 32.3 mm) of a 41-year-old woman. Ovality index (maximum diameter/minimum diameter of the optic disc) is 2.36. (**g**, **h**) Examples of extremely tilted optic discs

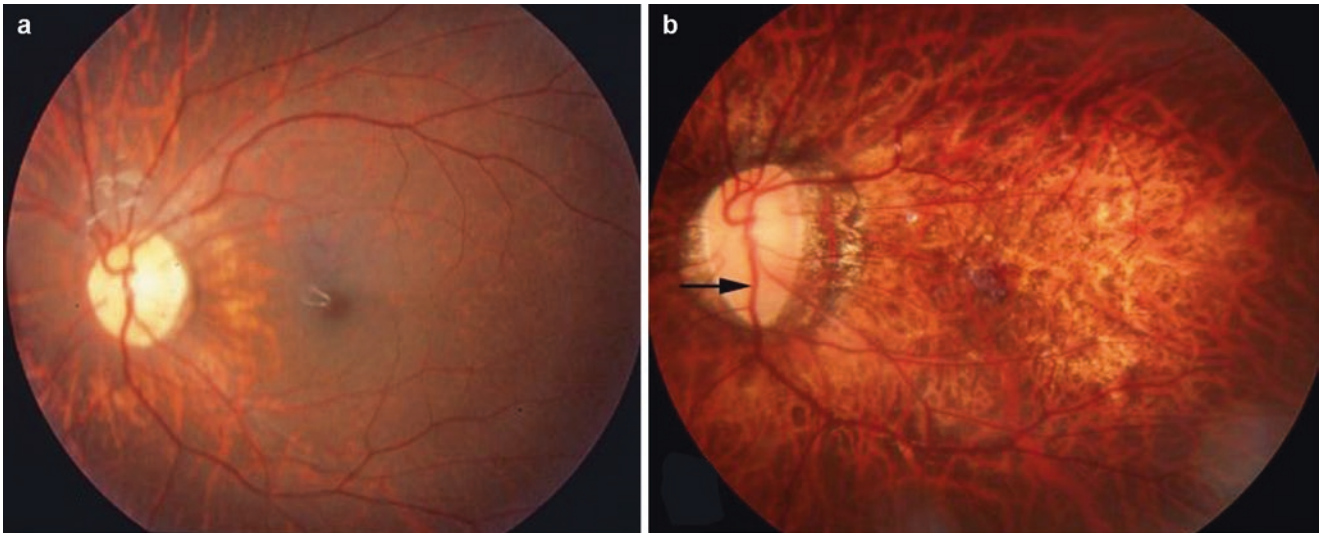

Fig. 25.4 Development of acquired megalodisc in a highly myopic patient with age. (**a**) The left fundus of an 8-year-old boy shows a slightly oval disc. Axial length is 27.96 mm. (**b**) Twenty-four years later, the optic disc is vertically elongated and becomes megalodisc like. Axial length increases to 31.11 mm. The optic disc area was 5.96 mm^2. Over the 24-year follow-up, there is vertical elongation of the disc. Note the retinal vein coursing on the optic disc (arrow) shows bifurcation at the disc border in (**a**) but is within the disc area in (**b**)

Fig. 25.5 (**a**) The right fundus of a 14-year-old boy shows almost round optic disc. (**b**) Twenty-two years later, the optic disc shows enlargement and torsion

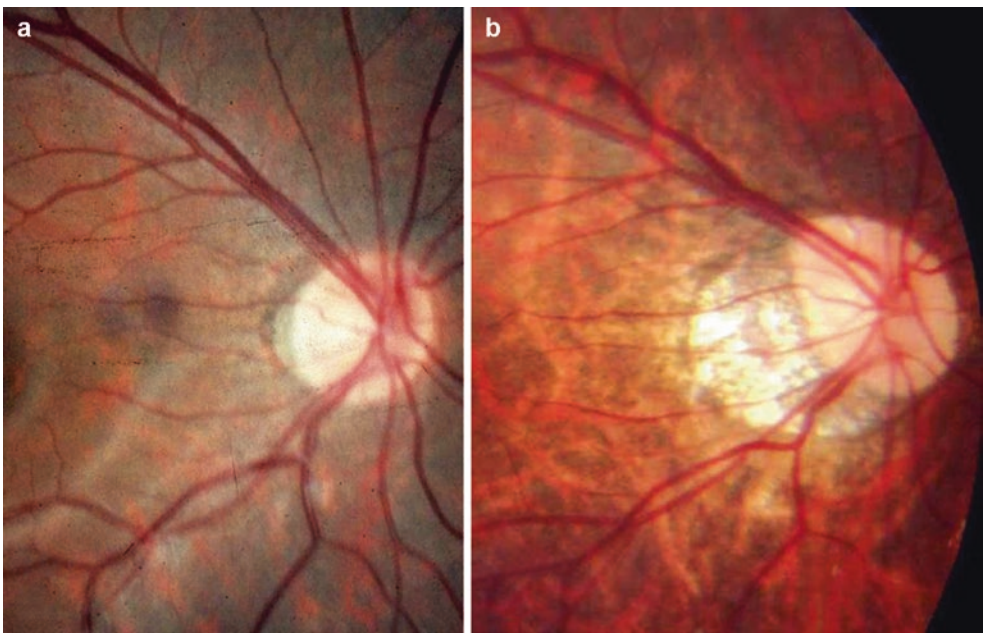

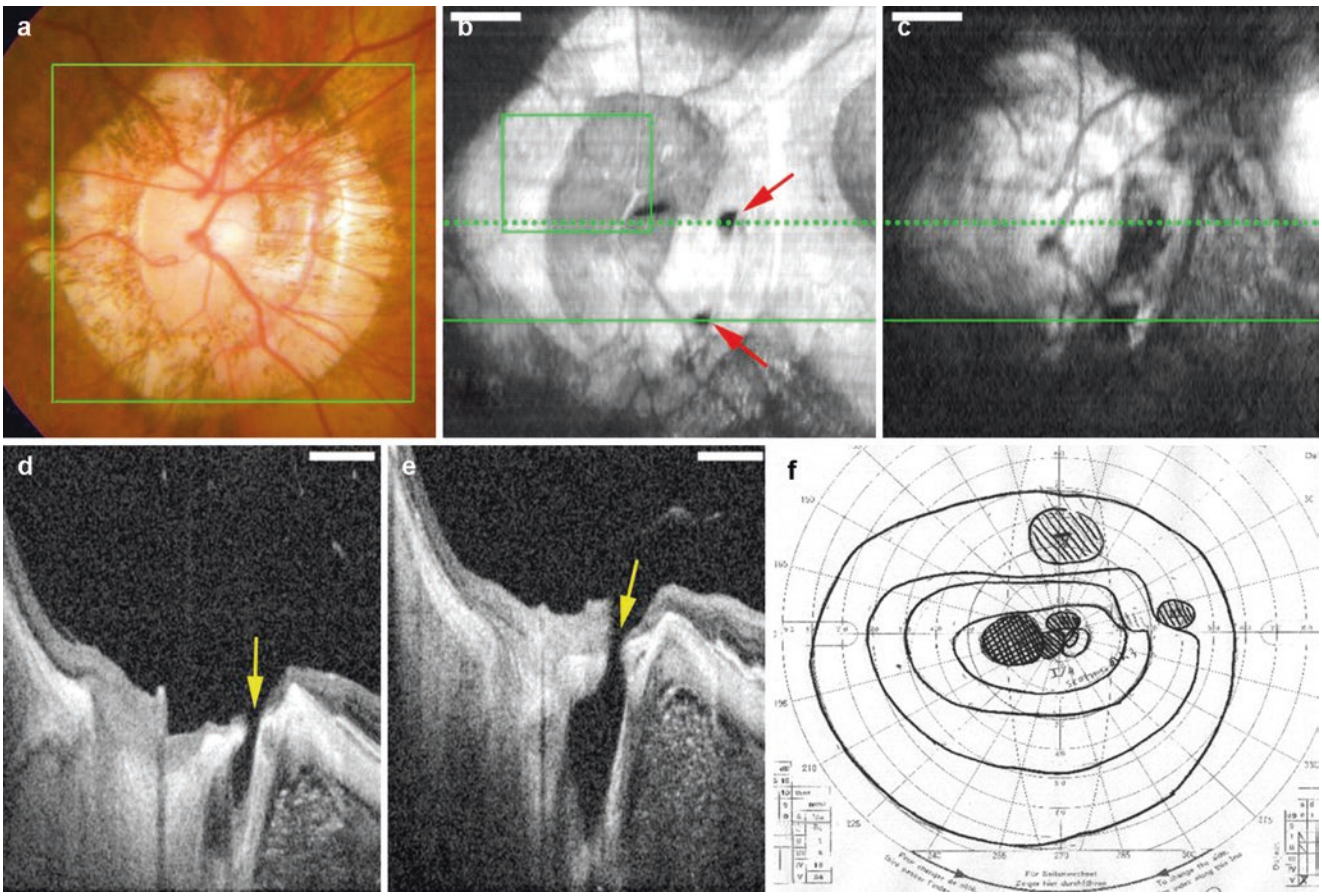

Fig. 25.6 Fundus photograph and swept-source OCT images showing deep pits extending toward the subarachnoid space (SAS). (**a**) Color fundus photograph of the optic disc showing a large annular conus. (**b**, **c**) En face cross-sectional images scanned in the area shown by the green square in (**a**). These en face images are from different levels and show that there are two pit-like pores (arrows) at the temporal border of the optic disc (**b**) and that these pores extend toward the SAS (**c**). (**d**, **e**) B-scan images acquired by 3D scan protocol showing the pits (arrows) extending toward the SAS; it is likely that there may be a direct communication with the SAS. (**f**) Visual fields from Goldmann perimetry show a central and a paracentral scotoma in addition to the nasal step. Scale bar, 1 mm

ever, there is not enough data at present to be certain of what proportion of tilted discs are congenital.

Samarawickrama and coworkers examined retinal images of 1765 children aged 6 years and found 20 (1.6%) had tilted discs [53]. In these children, there was no association with myopia. A similar study in adolescent children in Singapore found tilted optic discs in 454 (37%) of 1227 children with a mean age of 14 years, and there was a very strong association with myopia [54]. Except for 20 cases, all eyes with tilted optic nerve had beta zone peripapillary atrophy. In the Blue Mountains study, which some of the same authors participated [40], tilted discs were found in 56 subjects among 3583 adult participants, or 1.6%. The proportion of eyes with tilted discs was much greater among adult eyes with high myopia. The authors concluded the similar prevalence was evidence that tilted optic discs are really congenital. On the other hand, Kim and colleagues documented how the tilted appearance occurs over time in children [55], including the development of alteration in the shape of the optic disc. Patients with unilateral myopia have tilted discs only or, more prominently, in the myopic eye. Therefore, some tilted discs may be a function of morphogenic changes of the eye wall contour that occur in the development of high myopia, such as staphyloma formation. Another interesting take on this data is some patients have identifiable traits early when they are not myopic that may be predictive of high myopia later in life. The true estimation of the proportion of congenital tilted discs would be obtained from examining babies.

The retinal nerve fibers in a highly myopic eye still converge on the optic canal, but the path taken by the fibers is different in a highly myopic eye with a tilted disc. The shifting of the layers, particularly of the opening in Bruch's membrane in relationship to the scleral opening, was readily known to ophthalmologists in the nineteenth century [56, 57]. With the advent of high-resolution OCT, the changes seen in gross specimens can now be seen in vivo. There is a shift of the Bruch's membrane opening over the scleral canal in the temporal direction, so the nasal aspect of Bruch's

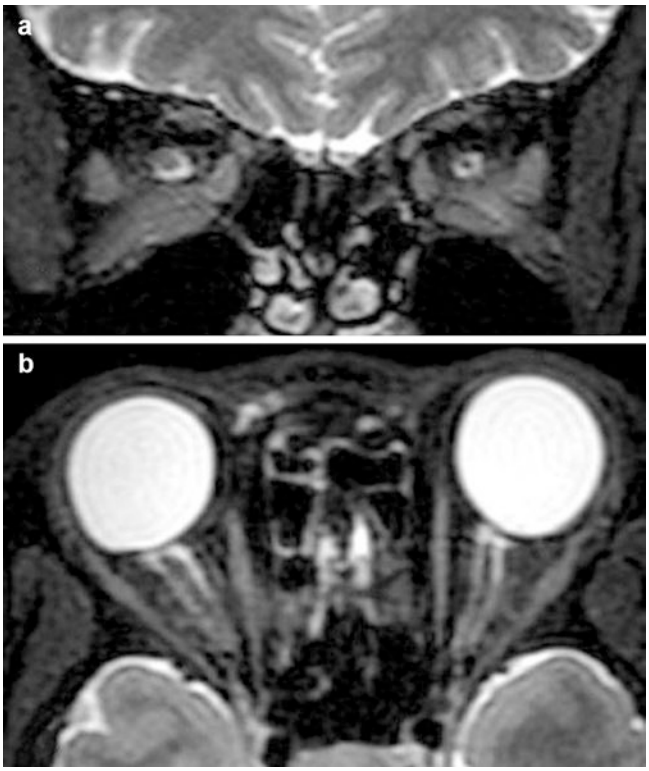

Fig. 25.7 Dilation of subarachnoid space (SAS) shown as ring sign in MRI images. (**a**) Coronal section of T_2-weighted MRI image showing a ring sign to show a dilated SAS around the optic nerve. (**b**) Horizontal section showing a tram track sign along the retrobulbar optic nerve

membrane appears to "slice" into the nasal aspect of the tilted nerve. The nasal border of the nerve, as defined by the Bruch's membrane opening, is often much more temporal than would be appreciated by cursory ophthalmoscopy. This causes the nasal retinal nerve fibers to make a sharp hairpin turn to enter the optic nerve. This was called "supertraktion" by German ophthalmologists and "supertraction" or "supertraction crescent" by the English [56–58]. On the temporal side of the nerve, the absence of tissue was called the "distraction crescent" [59], signifying the pulling away of tissue by shifting tissue planes. The temporal retinal nerve fibers enter the tilted nerve at an angle greater than 90 degrees. Tilted discs are often associated with inferior staphylomas, which are discussed in Chaps. 8 and 13.

Eyes with tilted discs commonly have visual field defects, which typically are arcuate. The most common is a bitemporal arcuate defect that does not respect the midline. This feature helps rule out the possibility of a chiasmal disorder. The arcuate-shaped defects also do not necessarily respect the horizontal midline, a finding uncommon in early glaucoma. Vongphanit and associates found the mean spherical refraction in eyes with titled optic disc and visual field defects was −5.6 diopters [60], but visual field defects associated with tilted discs do not necessarily occur in eyes that are highly myopic or even myopic at all [60–62]. In agreement with the original article by Young [61], the most common location was superotemporal. The blind spot also may be enlarged and is usually proportional to the area of atrophy related to the conus. In the original description of tilted disc syndrome in 1976, one cause for the superior field defects was considered to be the "variable myopia" caused by "localized staphylomatous ectasia" [61]. Prior to being called tilted disc syndrome, earlier authors described similar eye configurations using terms such as situs inversus of the optic disc with inferior conus [62–66]. These authors noted the variable myopia and the ability to cause the visual field defect to disappear by changing the refraction [63, 65], an observation reported again decades later [67]. In inferior staphyloma, the eye wall bulges out posteriorly inferiorly, and as a consequence the image plane lies increasingly in front of the retina. The sensitivity of the retina is dependent on the illuminance, the luminous flux incident per unit area of the photoreceptors. A defocused image spreads the same number of photons of light over a larger area thus potentially reducing the sensitivity to threshold change. Altering the refraction in front of the eye can make visual field defects disappear in some eyes with inferior staphylomas. Even though this effect appears to be well known, as it was described repeatedly since the 1950s, reported studies in which the correction was actually done are rare. Therefore, it is likely many reported studies of visual field defects in tilted disc syndrome may be related to refractive abnormalities. However Young and coworkers stated not every patient had a staphyloma [61], and Hamada and coworkers found the visual field defects frequently did not correlate with the anatomic changes in the eye [68]. Odland et al. reported that stronger myopic correction could decrease the scotoma but in their patients did not cause it to completely disappear [65]. So there must be additional reasons for the field defects. These eyes can show alterations of the critical fusion frequency [69], and electroretinographic abnormalities to include the multifocal electroretinogram [68, 70, 71], and reduced visual evoked responses [68]. Nevertheless some of these abnormalities were attributed to locally defocused images by the respective authors. Some of the pathophysiologic causes have proposed and include hypoplasia of the retina and choroid with subsequent distortion of structures around the disc [63], altered retinal pigment epithelium, and choroidal atrophy [66].

The visual field defects in tilted disc syndrome are generally stable, which can be a help in ruling out a concurrent diagnosis of glaucoma. The visual fields are not stable in all high myopes. Carl Stellwag von Carion noted in the nineteenth century that staphylomas appeared to be acquired and they progressed, sometimes very slowly, over a period of many years [72]. To the extent the visual field defects are related to staphylomas, either because of refractive or physi-

ologic reasons, there is a possibility with long-term follow-up the visual field may progress. In highly myopic patients who showed VF defects which are not explained by myopic fundus lesions, Ohno-Matsui and coworkers performed multiple regression analyses to determine the correlations between the visual field score and these possible factors: age at the initial examination, age at the last examination, axial length, initial IOP, mean IOP during the follow-up, maximum to minimum diameter measurements of the optic disc, and the presence of an abrupt change of scleral curvature temporal to the optic disc [73]. The results showed that the presence of an abrupt change of scleral curvature temporal to the optic disc was the only factor which correlated with a progression of visual field defects in highly myopic patients [73]. In addition to all of the previously mentioned theories for decreased sensitivity, the findings of this study raise new possibilities. One is that the sharp bend in the sclera may put mechanical stress on the nerve fiber to potentially cause injury. Second, there is the possibility of the Stiles-Crawford effect playing a role, since the tilted photoreceptors would be expected to have a reduced response. Akagi and coworkers found the retinal nerve fiber thickness was inversely related to the angle the fibers had to take to hug scleral protrusions near the optic disc [74]. This finding may be a proxy for the curvature of the associated staphyloma. When considering the possibility of glaucoma, confirmatory evidence from retinal nerve fiber thickness measurements can be helpful. The pattern of retinal nerve fiber distribution is altered in tilted disc syndrome with thinner average; superior, nasal, and inferior but thicker temporal nerve fiber thicknesses; and a temporal shift in the superior and inferior peak locations [75, 76]. Eyes with tilted optic nerves generally show more tilt with greater amounts of myopia, and eyes with more tilting have a greater temporal shift in nerve fiber thickness measurements. Nerve fiber measurements in these eyes can be difficult and unreliable because of defects in segmentation, peripapillary atrophy, and schisis within the nerve fiber layer.

Torsion of the disc occurs when the ovoid of the optic nerve head is rotated in the coronal plane. More commonly this rotation is counterclockwise when viewing the right eye such that the superior aspect of the long axis is rotated temporally. The direction of optic disc torsion is a strong predictor of visual field defect location in normal-tension glaucoma [77]. There is a correlation between the amount of torsion and the visual field defect severity [78]. The retinal nerve fibers from the temporal periphery course around the central macula, apparently so they do not pass directly over the fovea. This diverts fibers to the superior and inferior nerve head. The retinal nerve fibers from the superior and inferior macula follow the analogous routes, respectively. Therefore, a large number of nerve fibers converge on the optic canal either superiorly or inferiorly. Rotation of the nerve would be expected to cause a shift of nerve fibers entering the nerve. In the Chennai Glaucoma Study [79] nerves showing outward rotation of the superior aspect of the nerve had thicker superior optic rims. In a study by Park and coworkers myopes with normal tension glaucoma were much younger than non-myopes and the biggest predictor of their visual field defects were the direction of optic nerve torsion [77]. Torsion of the nerve is much more common than is simple tilting. Some authors have used the term tilted to refer to both tilt and torsion. The remaining axis about which the optic disc potentially could rotate would cause deviation in the sagittal plane. This would produce a difference in elevation of the superior aspect of the disc in relation to the inferior portion. Given that inferior staphylomas are common, the inferior portion of the disc is commonly more posterior.

25.8 Optic Neuropathy Associated with Optic Nerve Abnormalities That May Not Be Progressive

Doshi and coworkers [80] described a group of young to middle-aged men of Chinese origin who had optic nerve cupping and visual field abnormalities suggestive of glaucoma, but they had stable ocular findings for up to 7 years. The authors hypothesized that during the ocular expansion and associated deformation of the lamina cribrosa and altered entry angles for retinal nerve fibers may have put undue stress on some of the nerve fibers. The authors hypothesized that loss of these nerve fibers would lead to cupping and field loss, but with stabilization of myopic expansion, the process may not be progressive. The follow-up period, even though it was up to 7 years, does not mean the subjects would not show visual field progression, particularly in later years when glaucoma is much more common. Of interest is that analysis of 26 eyes of 26 young myopic primary open-angle glaucoma patients with progressive optic disc tilting showed an associated visual field mean deviation worsening [81].

25.9 Optic Disc Abnormalities Associated with Generalized Expansion

While it would seem to be an easy research question to answer, the exact relationship between axial length, myopia, and disc size is still a matter of contention. A histogram of proportion of the population tested versus refractive error shows a nearly normal distribution, albeit one skewed to the right. For most eyes, that is those having a refractive error somewhere between low grades of hyperopia to moderate amounts of myopia, there is little to no significant relationship between refractive error (or the corresponding axial length) and disc area [82–89]. There is a clear relationship for eyes with high amounts of myopia and disc area. These

eyes represent a small proportion of the general population and show values clearly different than the rest of the data. In a sense, highly myopic eyes are outliers and when included with the rest of the population can influence the overall correlation between refractive error and disc size. The Rotterdam Eye study reported a 0.033 mm^2 increase in disc area with each diopter of refractive error [16]. Even if this were applicable to lower grades of myopia, the increase in disc area is very small. However among highly myopic eyes, particularly those with a refractive error greater than – 8 diopters, the disc area increases substantially in size [85, 86]. Two groups of investigators using OCT thought there was an inverse correlation between optic disc size and either refractive error or axial length, but the authors did not appear to perform any image size corrections for magnification variations [90, 91].

Optic discs in normal eyes show significant variation is size, independent of refractive error. Discs much larger than typical are called macrodiscs. For the Beijing Eye study, the calculated threshold was 3.79mm^2 [85]. Eyes with macrodiscs generally fall into one of two classes. One is termed primary macrodisc in which the size of the disc does not appear to bear any relationship to refractive error. In secondary, or acquired, macrodisc, the optic nerve enlargement is associated with myopia, generally a refractive error of −8 or greater. Macrodiscs associated with myopia typically show generalized enlargement, but this enlargement may not necessarily be isotropic. As a consequence, it is possible to see discs that are distorted in shape as well as being large. Macrodiscs typically have a flattening of the cup with reduced optic disc rim thickness and consequently increased cup/disc metrics. These discs may also appear somewhat pallorous as compared with normal discs in emmetropes. The macrodiscs not related to myopia generally do not show pallor or flattening of the disc and they have deeper cups. Along with the generalized enlargement of the disc, there are associated thinning of the adjacent sclera and development of pits in the nerve and adjacent sclera.

The peripapillary region in eyes with megadiscs secondary to high myopia invariably have prominent peripapillary atrophy that involves the choroid, RPE, and outer retina. In some eyes, there can be marked thinning or even frank defects of the nerve fiber layer. In these eyes the segmentation routines used to detect retinal nerve fiber layer thickness break down and consequently do not accurately measure the thickness of the retinal nerve fiber layer. These are the patients that are among the most difficult to evaluate for glaucoma. Under the best of circumstances, the optic disc in high myopia with disc enlargement may have a smaller rim, the disc is usually pale, visual field testing shows at least an enlargement of the blind spot, and retinal nerve fiber layer measurements are not reliable. Patients with very high amounts of myopia have depressed threshold sensitivities. There are potential difficulties with retinal nerve fiber layer analysis in high myopes; an alternative measurement could be to measure the cell bodies instead of the axons. The ganglion cell complex can be visualized, segmented, and measured in eyes and has been proposed as a method to help diagnose and follow glaucoma in highly myopic eyes [92–94]. The area under the curve for ganglion cell complex measurements appears as good as or better than nerve fiber layer measurements. There is disagreement about parameter variation and myopia with this newer modality. Shoji and coworkers [93] found no association between thickness and amount of myopia while Zhao and Jiang did [94].

25.9.1 Dilation of Perioptic Subarachnoid Space and Thinning of Peripapillary Sclera

Expansion of the subarachnoid space (SAS) near the exit of the optic nerve has been noted more than 100 years ago [95–100]. The terminology used then was a bit different than today. The subarachnoid space was seen to end in a blind pouch that was thought to be bounded by scleral fibers that were confluent with the termination of the arachnoid and the dura, which themselves merged together. The space was called the intervaginal space by many authorities, and others called it the subarachnoid space. The space was seen to be enlarged in cases of infection because of increased intracranial pressure, tumor, optic atrophy, and in myopia. First described by von Jaeger, early ideas were that the expansion of the space was due to ocular expansion during myopia development, Schnabel considered the enlargement a congenital abnormality that occurred in eyes that also commonly developed myopia, while Landolt thought the expansion of the dural insertion caused weakness of the posterior portion of the eye with staphyloma development as a consequence [100]. In myopic eyes with an enlarged intervaginal space, the sclera was seen to be exceedingly thin by a number of authorities of that age and was described by Parsons as leaving only a “few layers of scleral lamellae” [99]. Okisaka [101] reported that in emmetropic eyes, the perioptic SAS was narrow and the SAS blindly ended at the level of lamina cribrosa. The dura of the SAS was attached to the peripapillary sclera just around the lamina cribrosa. In contrary, in highly myopic eyes, the perioptic SAS was enlarged together with an increase of the axial length (Fig. 25.7).

Observations by investigators such as Okisaka and Jonas [102, 103] have helped refine concepts of the enlargement of the subarachnoid space and associated histologic changes in the posterior eye wall. Jonas found that the scleral flange, the distance between the optic nerve border, and the attachment of the dura to the sclera were correlated with increased axial length and inversely correlated with the scleral thickness

[102]. The scleral flange thickness was seen to be attenuated in myopic eyes, with some having thicknesses of less than 100 microns [103]. Over the course of more than a century, observations of the perioptic subarachnoid space were typically made on autopsy eyes.

In T_2 images of MRI, the dilated SAS around the optic nerve can be observed as a ring sign, which is somewhat similar to the findings seen in patients with increased intracranial pressure (Fig. 25.7). Enhanced depth imaging (EDI)-OCT and swept-source OCT provided deeper imaging capabilities as compared with conventional spectral domain (SD) OCT and made it possible to visualize the deeper structures in detail in vivo. Park et al. [104] used EDI-OCT and observed the SAS around the optic nerve in 25 of the 139 glaucomatous eyes (18%). Most of the 25 eyes had high myopia and extensive parapapillary atrophy. Ohno-Matsui and coworkers [105] used swept-source OCT and visualized a dilated SAS in 124 of 133 highly myopic eyes (93.2%) but could not visualize the SAS in the emmetropic eyes. The SAS was triangular, with the base toward the eye surrounding the optic nerve (Fig. 25.5) and it contained a branching internal structure. The attachment of the dura to the eye wall could be clearly seen offset from the immediate peripapillary area, and there was a change in the scleral curvature at the site of attachment. In one highly myopic eye, there appeared to be a direct communication between the intraocular cavity and SAS through pit-like pores (Fig. 25.6).

The expanded area of exposure to CSF pressure along with thinning of the posterior eye wall may influence staphyloma formation and the way in which diseases may be manifested. Marcus Gunn stated that he rarely saw optic nerve swelling in high myopes with brain tumors [106]. While he stated the joint probability of the two was low, he proposed the excessive cerebrospinal fluid pressure in the subarachnoid space may be spread out over a larger area of the posterior portion of the eye or may be locally dissipated by the thinned dura near the eye in highly myopic eyes. There may in fact be weakening of the ocular wall, as Landolt suggested [96], but the amount of staphyloma formation would be influenced by not only the thinning of the sclera but also by the alteration in trans-scleral forces caused by the wider region of exposure to the cerebrospinal fluid pressure. Many questions remain unanswered but potentially could be modeled now that imaging techniques are capable of visualizing these areas.

25.9.2 Formation of Acquired Pits in the Optic Disc and Conus Regions

Because of the expansion of the posterior portion of the globe, scleral emissaries can show remarkable expansion in size as shown in Chap. 8. Similar expansion of the region centered on the nerve can cause several broad classes of analogous abnormalities (Fig. 25.8). Pit-like changes can be seen in the region of the conus similar to those in the macular region [107]. There can be clefts at the border of the optic nerve, which may be secondary to expansion-induced stress at this junction. Finally tears in the lamina cribrosa, similar to those seen in glaucomatous eyes, have been seen in highly myopic eyes, and these dehiscences may be associated with depressions or pits in the optic nerve [108]. By using swept-source OCT, Ohno-Matsui and colleagues [107] found pit-like clefts at the outer border of the optic nerve or within the adjacent scleral crescent in 32 of 198 highly myopic eyes (16.2%) but in none of the emmetropic eyes. The pits were located in the optic disc in 11 of 32 eyes (Figs. 25.9 and 25.10) and in the area of the conus outside the optic disc (conus pits) in 22 of 32 eyes. The nerve fiber tissue was discontinuous overlying the pits, and this discontinuity may be yet another reason for visual field defects in highly myopic patients. In some cases, the retinal vessels herniated into the

Fig. 25.8 Deeply excavated pit-like structures within the optic disc area in a highly myopic eye suspected of having glaucoma. The refractive error was −18.0 D and the axial length was 29.4 mm. Bar, 1 mm. (**a**) Right fundus of a 45-year-old woman shows an atrophic glaucomatous optic disc and temporal conus. The green arrows show the scanned lines of the swept-source OCT images shown in D and E. (**b**) Magnified view shows the large optic disc with saucerization. Note how the vessels inferiorly dip out of view at the inferior border of the disc indicative of cupping. The green lines are the scanned lines of the swept-source OCT images shown in F and G. (**c**) En face view of the optic disc reconstructed from three-dimensional images of swept-source OCT shows two large pits at the upper and lower poles of the optic disc (arrows). These pits have a triangular shape, and their bases are directed to the edge of the optic disc. Multiple pit-like structures are also observed along the temporal margin of the optic disc (arrowheads). (**d**) B-scan swept-source OCT image of the scanned line shown in (**a**) shows a deep pit (arrow) in the inferior pole of the disc extending posteriorly beyond the lamina cribrosa. The inner surface of the lamina is indicated by arrowheads. The nerve fiber overlying the pit is disrupted. (**e**) B-scan swept-source OCT image of the scanned line shown in (**a**) shows an oval-shaped, deeply excavated pit (arrow) at the superior pole of the optic disc with a wide opening. The lamina is dehisced from the peripapillary sclera at the site of the pit, and the nerve fibers overlying the pit are discontinuous at the pit. The depth of the pit from its opening is 1,142 μm. (**f**) B-scan swept-source OCT image across the scanned line shown in (**b**) shows a shallow pit (arrow) along the temporal margin of the optic disc. (**g**) Section adjacent to that shown in (**f**) shows a discontinuity of the lamina (arrow). A hyporeflective space is observed posterior to the defect

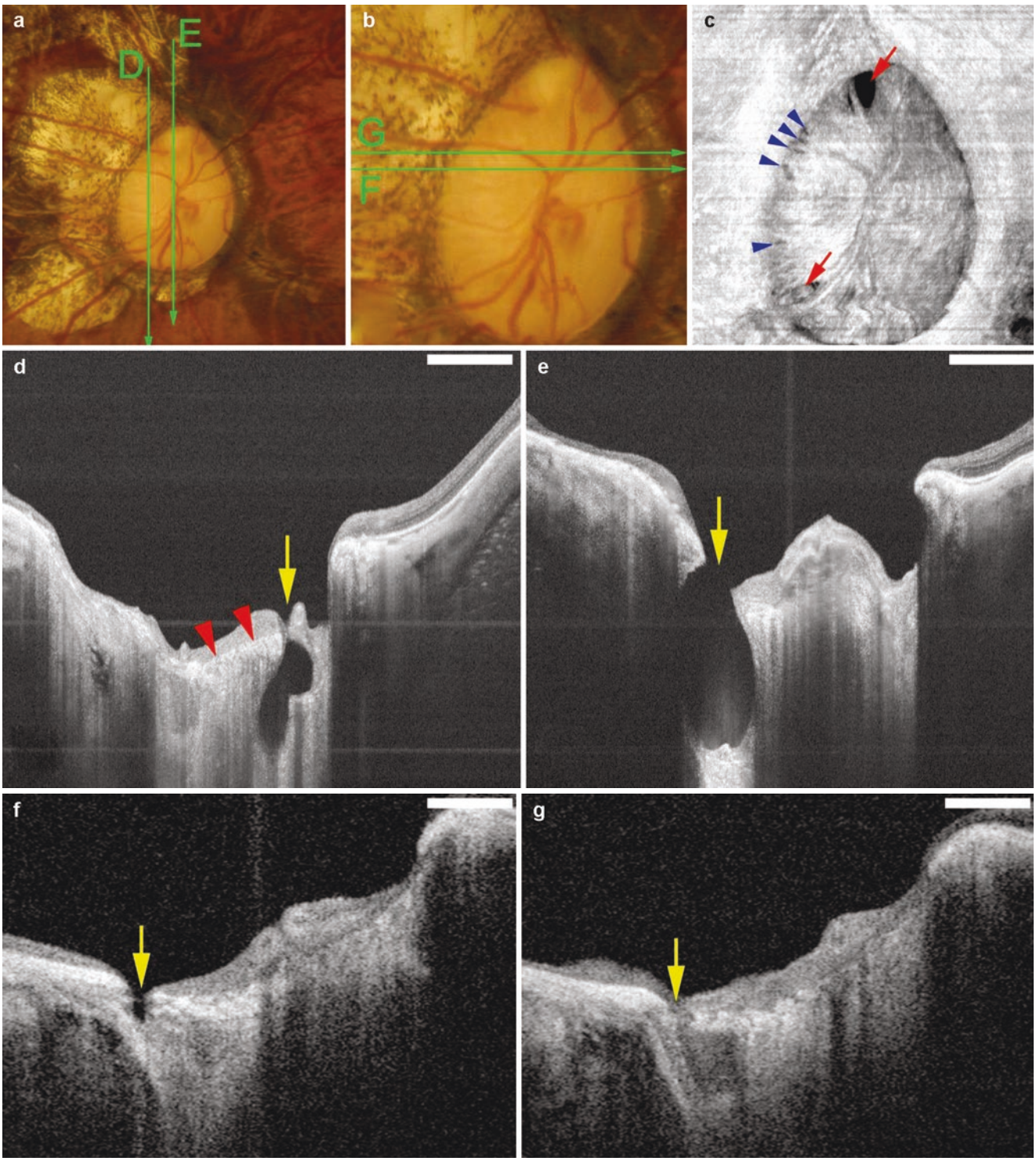
a
D
E
b
G
F
c
d
e
f
g

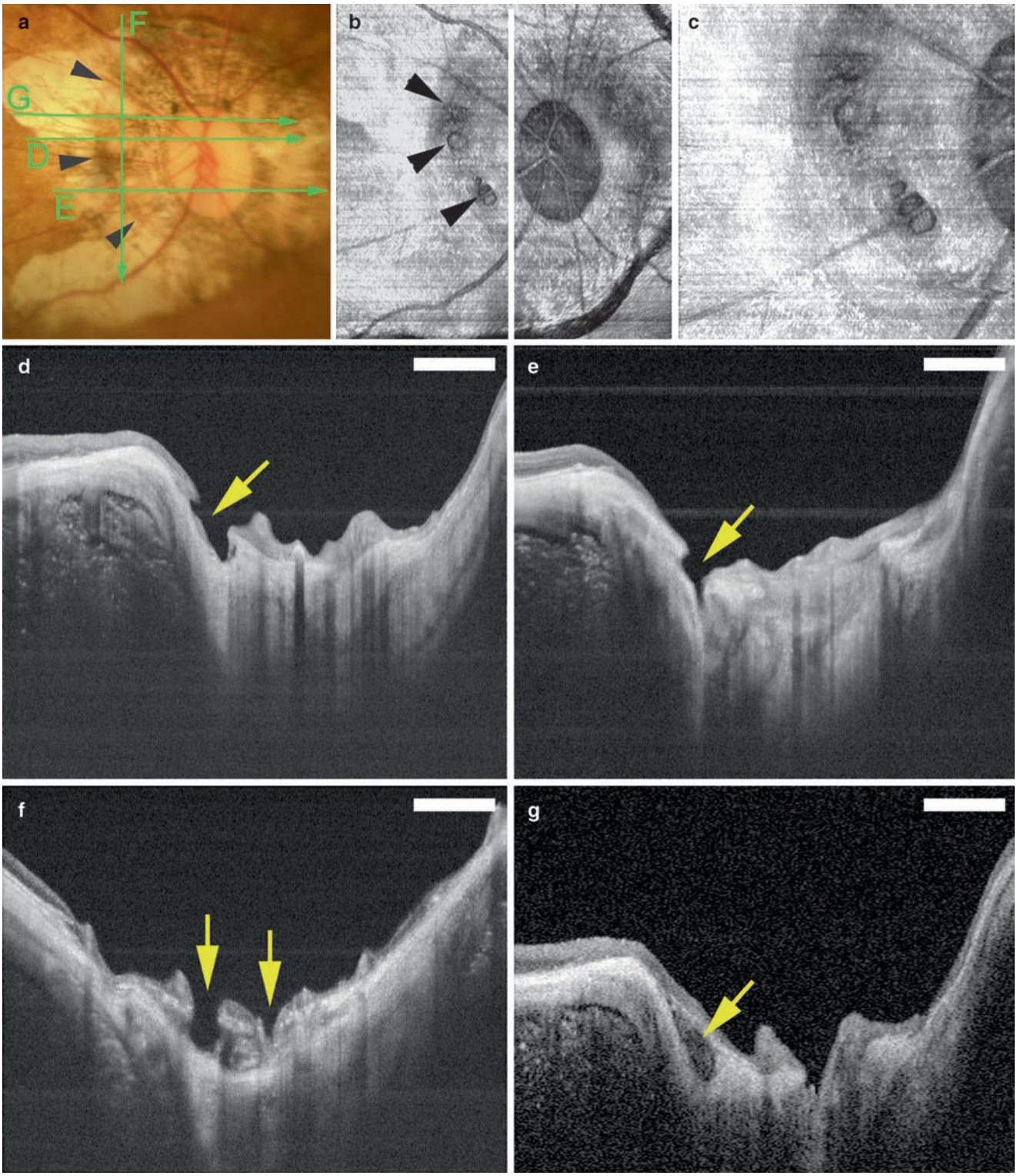

Fig. 25.9 Conus pits present on the temporal side of the scleral ridge in an eye with type IX staphyloma (Curtin's classification). The axial length of this eye was 32.8 mm with an intraocular lens implanted. Bar, 1 mm. (**a**) Photograph of right fundus of 64-year-old woman shows an oval disc with a large annular conus. A scleral ridge is shown by arrowheads. The green lines show the area scanned by swept-source optical coherence tomography (swept-source OCT) for the images shown in d through g. (**b**) En face image of the optic disc area reconstructed from three-dimensional swept-source OCT images shows multiple pits on the slope inside the ridge at approximately same distance from the optic disc margin (arrowheads). (**c**) Magnified view of (**b**) shows a collection of pits just temporal to the scleral ridge. (**d**) B-scan swept-source OCT image shows that the pit is present on the inner slope of the ridge (arrow). The peripapillary sclera and overlying nerve fiber tissue is discontinuous at the pit site. (**e**) Another pit can be seen inferotemporal to the optic disc. (**f**) Vertical OCT scan temporal to the optic disc shows multiple pits (arrows), and the tissue around the pits appears like a sclera schisis. (**g**) Swept-source OCT section adjacent to the pits shows a hyporeflective space resembling a scleral schisis (arrow). The defects appear to be interruptions in the nerve fiber layer

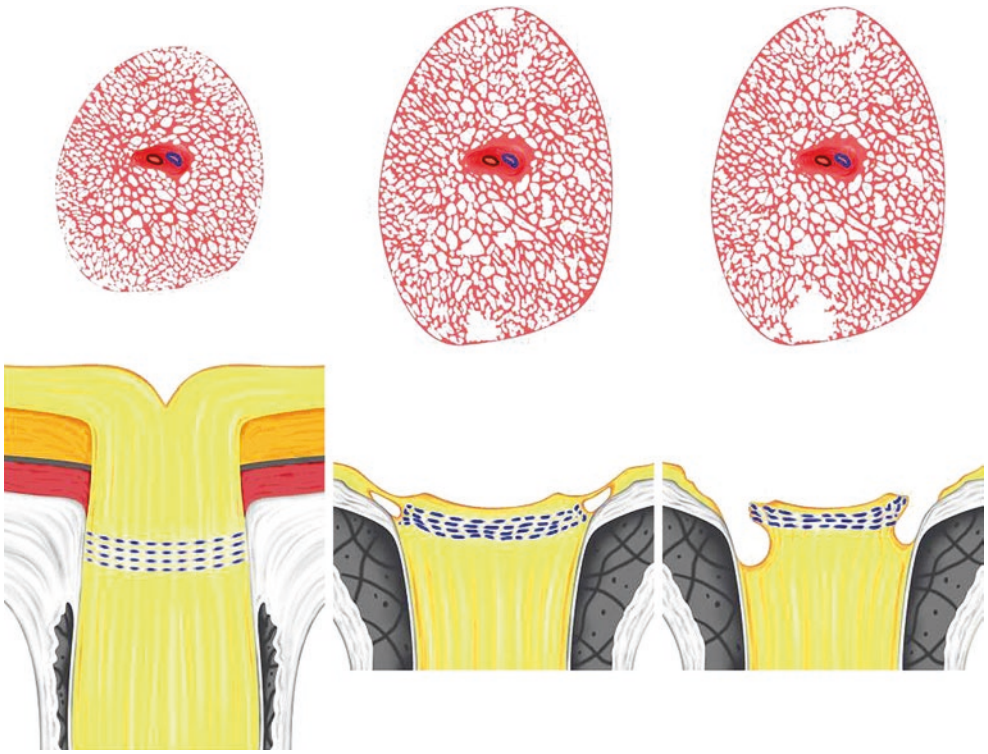

Fig. 25.10 Hypothetical scheme showing how optic disc pits develop. Upper panels show drawings of en face view of the optic disc and peripapillary area. Lower panels show cross-sectional images. The optic disc is first enlarged by a mechanical expansion of the papillary region (upper middle image). Because of the mechanical expansion, the lamina eventually dehisces from the peripapillary sclera particularly at the superior and inferior poles. This stage is observed by swept-source OCT as hyporeflective gap at the junction between the lamina cribrosa and the peripapillary sclera. With further increase of the size of the gap, the nerve fiber overlying this gap may be sunken, displaced, or disrupted, and this stage is observed as optic disc pits by swept-source OCT (lower right image)

conus pits. Schematic illustration of development of optic disc pits and conus pits are shown.

25.9.3 Separation of Circle of Zinn-Haller from the Optic Nerve

Because of its intrascleral location, it had been difficult to observe the circle of Zinn-Haller in situ. Thus, most of the studies of the circle of Zinn-Haller have been done using histological sections [10, 109] or vascular castings with methyl methacrylate [110–112] of human cadaver eyes. Expansion of the circle of Zinn-Haller and associated circulatory alterations were proposed to be a cause peripapillary choroidal atrophy in high myopia by Elmassri in 1971 [113]. Following identification of the circle of Zinn-Haller by angiography and Doppler ultrasonography [114], it was observed using fluorescein fundus angiography and indocyanine green (ICG) angiography in eyes with pathologic myopia with peripapillary atrophy (Fig. 25.11) [115–119]. EDI-OCT showed intrascleral cross sections of the vessels that were identified in ICG angiography images to correspond to the circle of Zinn-Haller. The filling of the circle of Zinn-Haller can be observed by ICG angiography to occur as would be expected by the known anatomy. In highly myopic eyes with large conus, the circle of Zinn-Haller had a horizontally long rhomboid shape, and the entry point of the lateral and/or medial short posterior ciliary arteries was at the most distant point from the optic disc margin. There are no currently known abnormalities correlated with the expansion of the circle of Zinn-Haller at present, but compromise in blood flow to the nerve may be a potential reason for the pallor sometimes seen in the optic disc of highly myopic eyes and also may be a contributing factor for the increased risk of glaucoma in highly myopic eyes. The increased radial distance between the expanded circle of Zinn-Haller in high myopes may decrease the blood perfusion into the nerve and may contribute to optic neuropathies such as glaucoma.

25.10 Eye Shape Abnormalities

Klein and Curtin, in their original description of lacquer cracks, sound a uniform constriction of the central fields, with a greater constriction to blue as compared with red test objects [120]. They thought the field defects were related to staphyloma formation and not the lacquer cracks. They also stated the increased constriction of the blue as compared

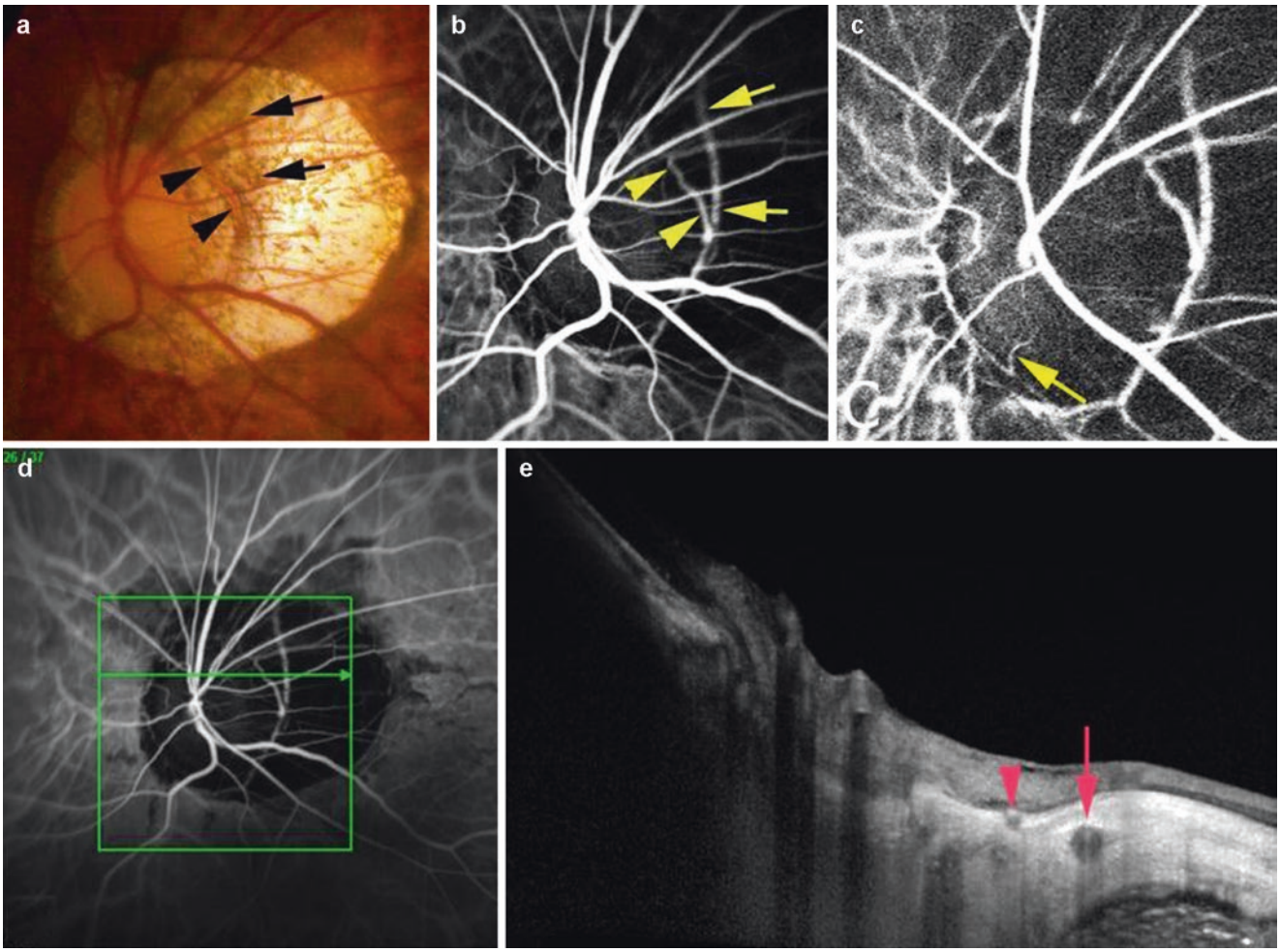

Fig. 25.11 Detection of Zinn-Haller arterial ring in a highly myopic patient by both indocyanine green (ICG) angiography and optical coherence tomography (OCT). (**a**) Fundus photograph of the left eye of a 60-year-old man with a refractive error of −11.25 D (spherical equivalent) and axial length of 28.4 mm. A large temporal conus is seen. Blood vessels suggesting the Zinn-Haller ring are seen within the conus (arrowheads). The vessels originating from short posterior ciliary arteries can also be seen (arrows). (**b**) ICG angiographic finding at 1 min after dye injection showing the Zinn-Haller ring (arrowheads) surrounding the optic disc in almost a circular shape. Vessels originating from the short posterior ciliary arteries can also be seen (arrows). (**c**) ICG angiographic image 12 s after the ICG injection showing the centripetal branch (arrow) running toward the optic nerve from the Zinn-Haller ring. (**d**) The scanned line by OCT (in bottom-right image) is shown on the ICG angiographic image. (**e**) Horizontal OCT scan shown as green line in bottom-left figure shows a cross section of the vessel of the Zinn-Haller ring as a small hyporeflective circle (arrowhead) near the inner surface of the peripapillary sclera. The vessel connecting the Zinn-Haller ring and retrobulbar SPCA is seen as a hyporeflective circle (arrow), which is wider and is situated deeper than the vessels of the Zinn-Haller ring

with the red test was a sign of retinal dysfunction [120]. Fledelius and Goldschmidt evaluated the eye shape and visual field abnormalities of the eyes with high myopia and found that abnormalities of both eye shape and visual field defects were more common with increasing myopia [121]. Moriyama and colleagues analyzed the shape of the human eye by using 3D MRI (see the "Staphyloma" chapter for details) [122]. The ocular shape as viewed from the inferior aspect of the eye was divided into distinct types, nasally distorted, temporally distorted, cylindrical, and barrel shaped. Statistical comparisons of the eyes showed that significant VF defects were found significantly more frequently in eyes with a temporally distorted shape. The area where the optic nerve is implanted in the globe was at the nasal edge of a temporal protrusion in these eyes. Thus, these eyes showed the presence of a change of the ocular shape just temporal to the optic disc. This corresponded to the stereoscopic fundus observation that eyes with a ridge-like protrusion just temporal to the optic disc tend to have VF defects significantly more frequently than eyes without the temporal ridge [74]. Using swept-source OCT to examine highly myopic eyes, Ohno-Matsui and coworkers analyzed the shape of sclera [123], which could be seen in its entire thickness. The curvatures of the inner scleral surface

of highly myopic eyes could be divided into those that were sloped toward the optic nerve, were symmetrical and centered on the fovea, were asymmetrical, and finally were irregular. Patients with irregular curvature were significantly older and had longer axial lengths than those with other curvatures. The subfoveal scleral thickness was significantly thinner in eyes with irregular curvature than the eyes with other curvatures. Myopic fundus lesions as well as visual field defects were present significantly more frequently in the eyes with irregular curvature. By comparison between OCT images and 3D MRI images, all of the eyes with temporally distorted shape by 3D MRI had irregular curvature by swept-source OCT. Combining these studies, the eye shape shown as temporally dislocated type by 3D MRI, irregular curvature by swept-source OCT, and steeply curved staphyloma visualized by stereoscopic fundus observation may be the same. While these changes in eye shape may induce local refractive variations, the same distortions also have the potential to put abnormal stresses on the retinal nerve fiber layer, and thus there could be a neurologic component. Future research will aim to clarify these questions. If eyes with these characteristics are found to have visual field defects, the likelihood is that visual field defects are due to local effects and not any type of optic neuropathy.

25.11 Myopic Optic Neuropathy

Since its earliest description, there has been controversy about the pathophysiology of glaucoma. Intraocular pressure may cause stress to the nerve fibers, particularly with elevated pressure. Intraocular pressure also appears to participate in remodeling of tissues such as the lamina cribrosa, which may compound the mechanical stress on nerve fibers. Another major group of hypotheses for glaucoma posits abnormalities in tissue perfusion as a cause of nerve fiber loss. Glaucoma is a neurodegenerative disease associated with specific ocular findings. Cupping in emmetropic eyes in relation to glaucoma is the result of loss of the nerve fibers and associated glial cells in the optic nerve head and to deformation of the lamina [124]. In pathologic myopia, the optic nerve head can show expansion, tilting, torsion, and effacement. All of these factors may put mechanical stress on the nerve fibers. Expansion of the circle of Zinn-Haller may also affect the perfusion into the nerve tissue. Pathologic myopes may develop an optic neuropathy that results in saucerization of the disc and visual field defects that resemble those seen in emmetropes with glaucoma. In a series of 155 patients in Korea [125] with normal tension glaucoma and asymmetric field loss, the eye with higher pressure in emmetropes showed more visual field loss. In myopes, refractive error, ovality index of the optic disc, and peripapillary atrophy were the predictors of visual field loss. This suggests there may be different pathophysiological reasons for visual field loss in emmetropes versus myopes in the eyes that do not demonstrate overtly elevated intraocular pressure, but both are the result of loss of nerve fibers. Is the diagnosis of glaucoma appropriate for all of these cases?

When evaluating a patient who may have glaucoma, one valuable test is visual field testing. In a study of 1434 visual field tests of 487 high myopes from a myopia registry, "arcuate-like" scotomata were found in 16.1%, advanced arcuate scotomata in 3.4%, nasal step in 5.1%, and enlarged blind spots in 25.6% [126]. Another common test is measuring the thickness of the retinal nerve fiber layer. This is often done in the parapapillary region with a circular scan. The distortion in pathologically myopic eyes places this circle at varying distances from the border of the optic nerve as compared with emmetropes. Therefore, the nomograms derived for emmetropic eyes does not apply to highly myopic eyes. A useful test in evaluating for possible glaucoma is the ganglion cell volume. This involves performing a volume scan of the macula followed by segmentation of the ganglion cell layer. This second step presents a challenge in highly myopic eyes. The distortion caused by staphylomata can lead to incorrect segmentation and image folding. Many image segmentation algorithms do not work if the eye has patchy atrophy. The lack of expected retinal layers obfuscates correct recognition of the remaining layers, yielding an incorrect result.

While tests used to diagnose glaucoma have a large variability, this is particularly true in pathologic myopia. A practical response is to examine repeated testing for signs of nerve fiber, ganglion cell, or visual field loss. If this can be demonstrated with certainty, the patient is often said to have glaucoma. This axiomatically leads to the only treatment for glaucoma, reduction in intraocular pressure. It may be possible that the numerous alterations in pathologic myopia have an unfavorable impact on retinal nerve fiber health by mechanisms that may overlap, but not be entirely the same as in "glaucoma," an admittedly nebulously defined disease. This second condition could be labeled myopic optic neuropathy. Under current levels of technology and understanding, this myopic optic neuropathy would be treated with reduction of intraocular pressure, even though we do not have good efficacy data.

25.12 The Need for Future Research

Patients with high myopia may have visual field defects, but how certain are we these defects are due specifically to the nerve and not to other coexistent abnormalities? We know that glaucoma is more common in eyes with myopia; it may be more difficult to diagnose glaucoma, particularly

in highly myopic eyes; and there may be changes in high myopia that emulate those occurring in glaucoma that may not, strictly speaking, be true glaucoma. There are undoubtedly altered mechanical stress on the nerve fibers and potential compromises in prelaminar perfusion. These considerations support the general idea that there may be types of optic neuropathy related to or accentuated by high myopia. There are many confounding factors that have not been fully evaluated. The interactions between expansion of the SAS, the myopic changes induced in the circle of Zinn-Haller, thinning sclera, and translaminar pressure are all variables that need closer examination. Many if not most of the visual field abnormalities also are associated with shape changes in the eye that directly or indirectly may cause decreased visual field performance independent of actual optic nerve abnormalities. The eye in myopia is longer, and as a consequence any test object of a given size will produce a larger image size on the retina, even if focused correctly. Since many eyes with abnormal visual fields also have abnormal shapes, there is a high likelihood of regionally varying focus. There is a complex aberration induced not necessarily by the dioptric mechanism of the eye, but by fluctuating deviations in distance of the retina from the image plane. This same expansion has the potential to cause regional variations in photoreceptor packing densities, as has been determined with adaptive optics imaging [127, 128]. The peripheral visual acuity is decreased in the periphery in myopes [129]. Deviation of the peripheral refraction from the measured central refractive error is much more pronounced in eyes with high myopia as compared with emmetropic eyes [130], and these alterations in peripheral refraction have potential to change the visual field test results. Coexistent with stretching of the wall of the eye is thinning of the choroid. Trying to determine the root cause of visual field defects in high myopia represents a significant challenge because of the many simultaneously changing variables, some known, some unknown, which coexist with any observed variable. Control, or at least measurement, of these simultaneously changing variables will be the only way to fully evaluate the contributions each of them make to visual field abnormalities in high myopia.

References

1. Stuermer CA, Bastmeyer M. The retinal axon's pathfinding to the optic disk. Prog Neurobiol. 2000;62(2):197–214.
2. Wang J, Liu G, Wang D, Yuan G, Hou Y, Wang J. The embryonic development of the human lamina cribrosa. Chin Med J. 1997;110(12):946–9.
3. Radius RL, Gonzales M. Anatomy of the lamina cribrosa in human eyes. Arch Ophthalmol. 1981;99(12):2159–62.
4. Quigley HA, Addicks EM. Regional differences in the structure of the lamina cribrosa and their relation to glaucomatous optic nerve damage. Arch Ophthalmol. 1981;99(1):137–43.
5. Park SC, Kiumehr S, Teng CC, Tello C, Liebmann JM, Ritch R. Horizontal central ridge of the lamina cribrosa and regional differences in laminar insertion in healthy subjects. Invest Ophthalmol Vis Sci. 2012;53(3):1610–6.
6. Zinn IG. Descripto Anatomica Oculi Humani. 1st ed. Gottingen: Abrami Vandenhoeck; 1755. p. 216–7.
7. Hayreh SS. Blood supply of the optic nerve head and its role in optic atrophy, glaucoma, and oedema of the optic disc. Br J Ophthalmol. 1969;53(11):721–48.
8. Lieberman MF, Maumenee AE, Green WR. Histologic studies of the vasculature of the anterior optic nerve. Am J Ophthalmol. 1976;82:405.
9. Jonas JB, Jonas SB. Histomorphometry of the circular peripapillary arterial ring of Zinn-Haller in normal eyes and eyes with secondary angle-closure glaucoma. Acta Ophthalmol. 2010;88(8):e317–22.
10. Ko MK, Kim DS, Ahn YK. Morphological variations of the peripapillary circle of Zinn-Haller by flat section. Br J Ophthalmol. 1999;83(7):862–6.
11. Zhao Y, Li F. Microangioarchitecture of the optic papilla. Jap J Ophthalmol. 1987;31:147–59.
12. Ruskell G. Blood flow in the Zinn-Haller circle. Br J Ophthalmol. 1998;82(12):1351.
13. Jonas JB, Gusek GC, Naumann GO. Optic disc, cup and neuroretinal rim size, configuration and correlations in normal eyes. Invest Ophthalmol Vis Sci. 1988;29(7):1151–8.
14. Quigley HA, Brown AE, Morrison JD, Drance SM. The size and shape of the optic disc in normal human eyes. Arch Ophthalmol. 1990;108(1):51–7.
15. Reis AS, Sharpe GP, Yang H, et al. Optic disc margin anatomy in patients with glaucoma and normal controls with spectral domain optical coherence tomography. Ophthalmology. 2012;119(4):738–47.
16. Ramrattan RS, Wolfs RC, Jonas JB, Hofman A, de Jong PT. Determinants of optic disc characteristics in a general population: the Rotterdam Study. Ophthalmology. 1999;106(8):1588–96.
17. Anderson DR. Ultrastructure of human and monkey lamina cribrosa and optic nerve head. Arch Ophthalmol. 1969;82(6):800–14.
18. Quigley HA, Coleman AL, Dorman-Pease ME. Larger optic nerve heads have more nerve fibers in normal monkey eyes. Arch Ophthalmol. 1991;109(10):1441–3.
19. Jonas JB, Schmidt AM, Müller-Bergh JA, Schlötzer-Schrehardt UM, Naumann GO. Human optic nerve fiber count and optic disc size. Invest Ophthalmol Vis Sci. 1992;33(6):2012–8.
20. Brodsky MC. Congenital Optic Disc Anomalies in Pediatric Neuro-Ophthalmology. New York: Springer; 2010. p. 59–67.
21. Quigley HA, Green WR. The histology of human glaucoma cupping and optic nerve damage: clinicopathologic correlation in 21 eyes. Ophthalmology. 1979;86:1803–30.
22. Quigley HA, Addicks EM, Green WR, et al. Optic nerve damage in human glaucoma. II. The site of injury and susceptibility to damage. Arch Ophthalmol. 1981;99:635–49.
23. Quigley HA, Hohman RM, Addicks EM, Massof RW, Green WR. Morphologic changes in the lamina cribrosa correlated with neural loss in open-angle glaucoma. Am J Ophthalmol. 1983;95(5):673–91.
24. Hernandez MR. Ultrastructural immunocytochemical analysis of elastin in the human lamina cribrosa. Changes in elastic fibers in primary open-angle glaucoma. Invest Ophthalmol Vis Sci. 1992;33(10):2891–903.
25. Fukuchi T, Sawaguchi S, Hara H, Shirakashi M, Iwata K. Extracellular matrix changes of the optic nerve lamina cribrosa in monkey eyes with experimentally chronic glaucoma. Graefes Arch Clin Exp Ophthalmol. 1992;230(5):421–7.
26. Fukuchi T, Sawaguchi S, Yue BY, Iwata K, Hara H, Kaiya T. Sulfated proteoglycans in the lamina cribrosa of normal mon-

key eyes and monkey eyes with laser-induced glaucoma. Exp Eye Res. 1994;58(2):231–43.
27. Hernandez MR, Yang J, Ye H. Activation of elastin mRNA expression in human optic nerve heads with primary open-angle glaucoma. J Glaucoma. 1994;3(3):214–25.
28. Park HY, Jeon SH, Park CK. Enhanced depth imaging detects lamina cribrosa thickness differences in normal tension glaucoma and primary open-angle glaucoma. Ophthalmology. 2012;119(1):10–20.
29. Quigley HA, Dorman-Pease ME, Brown AE. Quantitative study of collagen and elastin of the optic nerve head and sclera in human and experimental monkey glaucoma. Curr Eye Res. 1991;10(9):877–88.
30. Burgoyne CF, Downs JC, Bellezza AJ, et al. Three-dimensional reconstruction of normal and early glaucoma monkey optic nerve head connective tissues. Invest Ophthalmol Vis Sci. 2004;45:4388–99.
31. Downs JC, Yang H, Girkin C, et al. Three Dimensional histomorphometry of the normal and early glaucomatous monkey optic nerve head: neural canal and subarachnoid space architecture. Invest Ophthalmol Vis Sci. 2007;48:3195–208.
32. Yang H, Downs JC, Girkin C, et al. 3-D Histomorphometry of the normal and early glaucomatous monkey optic nerve head: lamina cribrosa and peripapillary scleral position and thickness. Invest Ophthalmol Vis Sci. 2007;48:4597–607.
33. Yang H, Downs JC, Bellezza AJ, et al. 3-D Histomorphometry of the normal and early glaucomatous monkey optic nerve head: prelaminar neural tissues and cupping. Invest Ophthalmol Vis Sci. 2007;48:5068–84.
34. Crawford Downs J, Roberts MD, Sigal IA. Glaucomatous cupping of the lamina cribrosa: a review of the evidence for active progressive remodeling as a mechanism. Exp Eye Res. 2011;93(2):133–40.
35. Mochizuki H, Lesley AG, Brandt JD. Shrinkage of the scleral canal during cupping reversal in children. Ophthalmology. 2011;118(10):2008–13.
36. Lee EJ, Kim TW, Weinreb RN. Reversal of lamina cribrosa displacement and thickness after trabeculectomy in glaucoma. Ophthalmology. 2012;119(7):1359–66.
37. Weiss AH. Unilateral high myopia: optical components, associated factors, and visual outcomes. Br J Ophthalmol. 2003;87(8):1025–31.
38. Weiss AH, Ross EA. Axial myopia in eyes with optic nerve hypoplasia. Graefes Arch Clin Exp Ophthalmol. 1992;230(4):372–7.
39. Fledelius HC, Goldschmidt E. Optic disc appearance and retinal temporal vessel arcade geometry in high myopia, as based on follow-up data over 38 years. Acta Ophthalmol. 2010;88(5):514–20.
40. Vongphanit J, Mitchell P, Wang JJ. Population prevalence of tilted optic disks and the relationship of this sign to refractive error. Am J Ophthalmol. 2002;133(5):679–85.
41. You QS, Xu L, Jonas JB. Tilted optic discs: the Beijing eye study. Eye (Lond). 2008;22(5):728–9.
42. How AC, Tan GS, Chan YH, Wong TT, Seah SK, Foster PJ, Aung T. Population prevalence of tilted and torted optic discs among an adult Chinese population in Singapore: the Tanjong Pagar study. Arch Ophthalmol. 2009;127(7):894–9.
43. Witmer MT, Margo CE, Drucker M. Tilted optic disks. Surv Ophthalmol. 2010;55(5):403–28.
44. Jonas JB, Gusek GC, Naumann GO. Optic disk morphometry in high myopia. Graefes Arch Clin Exp Ophthalmol. 1988;226(6):587–90.
45. Qiu M, Wang SY, Singh K, Lin SC. Association between myopia and glaucoma in the United States population. Invest Ophthalmol Vis Sci. 2013;54(1):830–5.
46. Dai Y, Jonas JB, Huang H, Wang M, Sun X. Microstructure of parapapillary atrophy: beta zone and gamma zone. Invest Ophthalmol Vis Sci. 2013;54(3):2013–8.
47. Suh MH, Na JH, Zangwill LM, et al. Deep-layer microvasculature dropout in preperimetric glaucoma patients. J Glaucoma. 2020;29(6):423–8.
48. Rudnicka AR, Edgar DF. Automated static perimetry in myopes with peripapillary crescents–part I. Ophthalmic Physiol Opt. 1995;15(5):409–12.
49. Rudnicka AR, Edgar DF. Automated static perimetry in myopes with peripapillary crescents–part II. Ophthalmic Physiol Opt. 1996;16(5):416–29.
50. Teng CC, De Moraes CG, Prata TS, Tello C, Ritch R, Liebmann JM. Beta-zone parapapillary atrophy and the velocity of glaucoma progression. Ophthalmology. 2010;117(5):909–15.
51. Jonas JB, Fernández MC, Naumann GO. Glaucomatous parapapillary atrophy. Occurrence and correlations. Arch Ophthalmol. 1992;110(2):214–22.
52. Tay E, Seah SK, Chan SP, Lim AT, Chew SJ, Foster PJ, Aung T. Optic disk ovality as an index of tilt and its relationship to myopia and perimetry. Am J Ophthalmol. 2005;139(2):247–52.
53. Samarawickrama C, Pai A, Tariq Y, Healey PR, Wong TY, Mitchell P. Characteristics and appearance of the normal optic nerve head in 6-year-old children. Br J Ophthalmol. 2012;96(1):68–72.
54. Samarawickrama C, Mitchell P, Tong L, et al. Myopia-related optic disc and retinal changes in adolescent children from Singapore. Ophthalmology. 2011;118(10):2050–7.
55. Kim TW, Kim M, Weinreb RN, Woo SJ, Park KH, Hwang JM. Optic disc change with incipient myopia of childhood. Ophthalmology. 2012;119(1):21–6.e1–3.
56. Jaeger E. Beiträge zur Pathologie des Auges 1870 Wien, Kaiserlich-Königliche Hof- und Staatsdruckerei, p202.
57. Heine L. Beiträge zur Anatomie des myopischen Auges. Arch f Augenheilk. 1899;36:277–90.
58. Siegrist A. Refraktion und akkomodation des menschlichen auges. Berlin, J. Springer 1925, p 111.
59. Collins ET, Mayou MS. An International System of Ophthalmic Practice. Pathology and Bacteriology. Philadelphia: P. Blakiston's Sone and Co; 1912. p. 505–7.
60. Vongphanit J, Mitchell P, Wang JJ. Prevalence and progression of myopic retinopathy in an older population. Ophthalmology. 2002;109(4):704–11.
61. Young SE, Walsh FB, Knox DL. The tilted disk syndrome. Am J Ophthalmol. 1976;82(1):16–23.
62. Caccamise WC. Situs inversus of the optic disc with inferior conus and variable myopia: a case report. Am J Ophthalmol. 1954;38(6):854–6.
63. Fuchs E. Uber den anatomischen Befund einiger angeborener Anomalien der Netzhaut und des Sehnerven. v. Graefes Arch. Ophthal. 1917;93:1–48.
64. Schmidt T. Perimetrie relativer Skotome. Ophthalmologica. 1955;129:303–15.
65. Odland M. Bitemporal defects of the visual fields due to anomalies of the optic discs. Acta Neurol Scand. 1967;43(5):630–9.
66. Traquair HM. Choroidal changes in myopia. In: Scott GI, editor. Traquair's clinical perimetry. 7th ed. London: Kimpton; 1957. p. 105–6.
67. Vuori ML, Mäntyjärvi M. Tilted disc syndrome may mimic false visual field deterioration. Acta Ophthalmol. 2008;86(6):622–5.
68. Hamada T, Tsukada T, Hirose T. Clinical and electrophysiological features of tilted disc syndrome. Jpn J Ophthalmol. 1987;31(2):265–73.
69. Feigl B, Zele AJ. Macular function in tilted disc syndrome. Doc Ophthalmol. 2010;120(2):201–3.
70. Giuffrè G, Anastasi M. Electrofunctional features of the tilted disc syndrome. Doc Ophthalmol. 1986;62(3):223–30.

71. Moschos MM, Triglianos A, Rotsos T, Papadimitriou S, Margetis I, Minogiannis P, Moschos M. Tilted disc syndrome: an OCT and mfERG study. Doc Ophthalmol. 2009;119(1):23–8.
72. Carl Stellwag von Carion. Treatise on the diseases of the eye, including the anatomy of the organ. [Translated by Roosa J, Bull CS, Hackley CE.] New York: William Wood and Co. 1873, pp 354–355.
73. Ohno-Matsui K, Shimada N, Yasuzumi K, Hayashi K, Yoshida T, Kojima A, Moriyama M, Tokoro T. Long-term development of significant visual field defects in highly myopic eyes. Am J Ophthalmol. 2011;152(2):256–265.e1.
74. Akagi T, Hangai M, Kimura Y, Ikeda HO, Nonaka A, Matsumoto A, Akiba M, Yoshimura N. Peripapillary scleral deformation and retinal nerve fiber damage in high myopia assessed with swept-source optical coherence tomography. Am J Ophthalmol. 2013;155(5):927–36.
75. Hwang YH, Yoo C, Kim YY. Myopic optic disc tilt and the characteristics of peripapillary retinal nerve fiber layer thickness measured by spectral-domain optical coherence tomography. J Glaucoma. 2012;21(4):260–5.
76. Hwang YH, Yoo C, Kim YY. Characteristics of peripapillary retinal nerve fiber layer thickness in eyes with myopic optic disc tilt and rotation. J Glaucoma. 2012;21(6):394–400.
77. Park HY, Lee K, Park CK. Optic disc torsion direction predicts the location of glaucomatous damage in normal-tension glaucoma patients with myopia. Ophthalmology. 2012;119(9):1844–51.
78. Lee KS, Lee JR, Kook MS. Optic disc torsion presenting as unilateral glaucomatous-appearing visual field defect in young myopic Korean eyes. Ophthalmology. 2014;121(5):1013–9.
79. Arvind H, George R, Raju P, Ve RS, Mani B, Kannan P, Vijaya L. Neural rim characteristics of healthy South Indians: the Chennai Glaucoma Study. Invest Ophthalmol Vis Sci. 2008;49(8):3457–64.
80. Doshi A, Kreidl KO, Lombardi L, Sakamoto DK, Singh K. Nonprogressive glaucomatous cupping and visual field abnormalities in young Chinese males. Ophthalmology. 2007;114(3):472–9.
81. Yoon JY, Sung KR, Yun SC, et al. Progressive optic disc tilt in young myopic glaucomatous eyes. Korean J Ophthalmol. 2019;33(6):520–7.
82. Britton RJ, Drance SM, Schulzer M, Douglas GR, Mawson DK. The area of the neuroretinal rim of the optic nerve in normal eyes. Am J Ophthalmol. 1987;103(4):497–504.
83. Varma R, Tielsch JM, Quigley HA, Hilton SC, Katz J, Spaeth GL, Sommer A. Race-, age-, gender-, and refractive error-related differences in the normal optic disc. Arch Ophthalmol. 1994;112(8):1068–76.
84. Rudnicka AR, Frost C, Owen CG, Edgar DF. Nonlinear behavior of certain optic nerve head parameters and their determinants in normal subjects. Ophthalmology. 2001;108(12):2358–68.
85. Wang Y, Xu L, Zhang L, Yang H, Ma Y, Jonas JB. Optic disc size in a population based study in northern China: the Beijing Eye Study. Br J Ophthalmol. 2006;90(3):353–6.
86. Xu L, Li Y, Wang S, Wang Y, Wang Y, Jonas JB. Characteristics of highly myopic eyes: the Beijing Eye Study. Ophthalmology. 2007;114(1):121–6.
87. Samarawickrama C, Wang XY, Huynh SC, Burlutsky G, Stapleton F, Mitchell P. Effects of refraction and axial length on childhood optic disk parameters measured by optical coherence tomography. Am J Ophthalmol. 2007;144(3):459–61.
88. Nangia V, Matin A, Bhojwani K, Kulkarni M, Yadav M, Jonas JB. Optic disc size in a population-based study in central India: the Central India Eye and Medical Study (CIEMS). Acta Ophthalmol. 2008;86(1):103–4.
89. Fledelius HC. Optic disc size: are methodological factors taken into account? Acta Ophthalmol. 2008;86(7):813–4.
90. Cheung CY, Chen D, Wong TY, Tham YC, Wu R, Zheng Y, Cheng CY, Saw SM, Baskaran M, Leung CK, Aung T. Determinants of quantitative optic nerve measurements using spectral domain optical coherence tomography in a population-based sample of non-glaucomatous subjects. Invest Ophthalmol Vis Sci. 2011;52(13):9629–35.
91. Knight OJ, Girkin CA, Budenz DL, Durbin MK, Feuer WJ, Cirrus OCT Normative Database Study Group. Effect of race, age, and axial length on optic nerve head parameters and retinal nerve fiber layer thickness measured by Cirrus HD-OCT. Arch Ophthalmol. 2012;130(3):312–8.
92. Kim NR, Lee ES, Seong GJ, Kang SY, Kim JH, Hong S, Kim CY. Comparing the ganglion cell complex and retinal nerve fibre layer measurements by Fourier domain OCT to detect glaucoma in high myopia. Br J Ophthalmol. 2011;95(8):1115–21.
93. Shoji T, Nagaoka Y, Sato H, Chihara E. Impact of high myopia on the performance of SD-OCT parameters to detect glaucoma. Graefes Arch Clin Exp Ophthalmol. 2012;250(12):1843–9.
94. Zhao Z, Jiang C. Effect of myopia on ganglion cell complex and peripapillary retinal nerve fiber layer measurements: a Fourier domain optical coherence tomography study of young Chinese persons. Clin Exp Ophthalmol. 2013;41(6):561–6. https://doi.org/10.1111/ceo.12045.
95. Donders FC. Die Anomalien der Refraction und Accommodation des Auges. Wein: Wilhelm Braumuller; 1866. p. 316.
96. Landolt E. Refraction and Accommodation of the Eye and their anomalies. [Translated by Culver CM]. Philadelphia: J. B. Lippincott Company. 1886; 432.
97. De Wecker L. Ocular Therapeutics. [Translated by Forbes L]. London, Smith Elder & Co. 1879, pp 413, 419.
98. Terrien F. Contribution a l'anatomie de loeil myope. Arch Ophtalmol. 1906:737–61.
99. Parsons JH. The pathology of the eye, vol. III. New York: G.P. Putnam's Sons; 1906.
100. Schnabel I (translated by Reed CH). The anatomy of staphyloma posticum, and the relationship of the condition to myopia. In, Norris WF, Oliver CA System of Diseases of the Eye. Part III. Local Diseases, Glaucoma, Wounds and Injuries, Operations. Philadelphia, J. B. Lippincott, 1900.
101. Okisaka S. Myopia. Tokyo: Kanehara Shuppan; 1987. p. 110–21.
102. Jonas JB, Berenshtein E, Holbach L. Lamina cribrosa thickness and spatial relationships between intraocular space and cerebrospinal fluid space in highly myopic eyes. Invest Ophthalmol Vis Sci. 2004;45:2660–5.
103. Jonas JB, Jonas SB, Jonas RA, Holbach L, Dai Y, Sun X, Panda-Jonas S. Parapapillary atrophy: histological gamma zone and delta zone. PLoS One. 2012;7(10):e47237. https://doi.org/10.1371/journal.pone.0047237.
104. Park SC, De Moraes CG, Teng CC, et al. Enhanced depth imaging optical coherence tomography of deep optic nerve complex structures in glaucoma. Ophthalmology. 2012;119:3–9.
105. Ohno-Matsui K, Akiba M, Moriyama M, et al. Imaging the retrobulbar subarachnoid space around the optic nerve by swept source optical coherence tomography in eyes with pathologic myopia. Invest Ophthalmol Vis Sci. 2011;52:9644–50.
106. Marcus Gunn R. Certain affections of the optic nerve. In, Ophthalmology. Essays, Abstracts and Reviews. Volume III. 1907(4): 253–269.
107. Ohno-Matsui K, Akiba M, Moriyama M, et al. Acquired optic nerve and peripapillary pits in pathologic myopia. Ophthalmology. 2012;119(8):1685–92.
108. Kiumehr S, Park SC, Syril D, et al. In vivo evaluation of focal lamina cribrosa defects in glaucoma. Arch Ophthalmol. 2012;130(5):552–9.
109. Jonas JB, Jonas SB. Histomorphometry of the circular peripapillary arterial ring of Zinn-Haller in normal eyes and eyes

with secondary angle-closure glaucoma. Acta Ophthalmol. 2010;88(8):1755–3768.
110. Olver JM, Spalton DJ, McCartney AC. Quantitative morphology of human retrolaminar optic nerve vasculature. Invest Ophthalmol Vis Sci. 1994;35(11):3858–66.
111. Olver JM, Spalton DJ, McCartney AC. Microvascular study of the retrolaminar optic nerve in man: the possible significance in anterior ischaemic optic neuropathy. Eye. 1990;4(Pt 1):7–24.
112. Morrison JC, Johnson EC, Cepurna WO, Funk RH. Microvasculature of the rat optic nerve head. Invest Ophthalmol Vis Sci. 1999;40(8):1702–9.
113. Elmassri A. Ophthalmoscopic appearances after injury to the circle of Zinn. Br J Ophthalmol. 1971;55(1):12–8.
114. Park KH, Tomita G, Onda E, Kitazawa Y, Cioffi GA. In vivo detection of perineural circular arterial anastomosis (circle of Zinn-Haller) in a patient with large peripapillary chorioretinal atrophy. Am J Ophthalmol. 1996;122(6):905–7.
115. Ohno-Matsui K, Morishima N, Ito M, et al. Indocyanine green angiography of retrobulbar vascular structures in severe myopia. Am J Ophthalmol. 1997;123(4):494–505.
116. Hollo G. Peripapillary circle of Zinn-Haller revealed by fundus fluorescein angiography. Br J Ophthalmol. 1998;82(3):332–3.
117. Ko MK, Kim DS, Ahn YK. Peripapillary circle of Zinn-Haller revealed by fundus fluorescein angiography. Br J Ophthalmol. 1997;81(8):663–7.
118. Ohno-Matsui K, Futagami S, Yamashita S, Tokoro T. Zinn-Haller arterial ring observed by ICG angiography in high myopia. Br J Ophthalmol. 1998;82(12):1357–62.
119. Yasuzumi K, Ohno-Matsui K, Yoshida T, et al. Peripapillary crescent enlargement in highly myopic eyes evaluated by fluorescein and indocyanine green angiography. Br J Ophthalmol. 2003;87(9):1088–90.
120. Klein RM, Curtin BJ. Lacquer crack lesions in pathologic myopia. Am J Ophthalmol. 1975;79(3):386–92.
121. Fledelius HC, Goldschmidt E. Eye shape and peripheral visual field recording in high myopia at approximately 54 years of age, as based on ultrasonography and Goldmann kinetic perimetry. Acta Ophthalmol. 2010;88(5):521–6.
122. Moriyama M, Ohno-Matsui K, Hayashi K, et al. Topographical analyses of shape of eyes with pathologic myopia by high resolution three dimensional magnetic resonance imaging. Ophthalmology. 2011;118(8):1626–37.
123. Ohno-Matsui K, Akiba M, Modegi T, et al. Association between shape of sclera and myopic retinochoroidal lesions in patients with pathologic myopia. Invest Ophthalmol Vis Sci. 2012;9:9.
124. Burgoyne C. The morphological difference between glaucoma and other optic neuropathies. J Neuroophthalmol. 2015;35 Suppl 1(0 1):S8–S21.
125. Lee EJ, Han JC, Kee C. Intereye comparison of ocular factors in normal tension glaucoma with asymmetric visual field loss in Korean population. PLoS One. 2017;12(10):e0186236.
126. Ding X, Chang RT, Guo X, et al. Visual field defect classification in the Zhongshan Ophthalmic Center-Brien Holden Vision Institute High Myopia Registry Study. Br J Ophthalmol. 2016;100(12):1697–702.
127. Kitaguchi Y, Bessho K, Yamaguchi T, et al. In vivo measurements of cone photoreceptor spacing in myopic eyes from images obtained by an adaptive optics fundus camera. Jpn J Ophthalmol. 2007;51:456–61.
128. Chui TY, Song H, Burns SA. Individual variations in human cone photoreceptor packing density: variations with refractive error. Invest Ophthalmol Vis Sci. 2008;49:4679–87.
129. Chui TY, Yap MK, Chan HH, Thibos LN. Retinal stretching limits peripheral visual acuity in myopia. Vis Res. 2005;45:593–605.
130. Atchison DA, Pritchard N, Schmid KL. Peripheral refraction along the horizontal and vertical visual fields in myopia. Vis Res. 2006;46(8–9):1450–8.